BIOTECHNOLOGICALLY RELEVANT ENZYMES AND PROTEINS

Comparison of CYP106A1 and CYP106A2 from *Bacillus megaterium* – identification of a novel 11-oxidase activity

Flora Marta Kiss[1] · Daniela Schmitz[1] · Josef Zapp[2] · Tobias K. F. Dier[3] ·
Dietrich A. Volmer[3] · Rita Bernhardt[1]

Abstract The CYP106A subfamily hydroxylates steroids, diterpenes, and triterpenes in a regioselective and stereoselective manner, which is a challenging task for synthetic chemistry. The well-studied CYP106A2 enzyme, from the *Bacillus megaterium* strain ATCC 13368, is a highly promising candidate for the pharmaceutical industry. It shares 63 % amino acid sequence identity with CYP106A1 from *B. megaterium* DSM319, which was recently characterized. A focused steroid library was screened with both CYP106A1 and CYP106A2. Out of the 23 tested steroids, 19 were successfully converted by both enzymes during in vitro and in vivo reactions. Thirteen new substrates were identified for CYP106A1, while the substrate spectrum of CYP106A2 was extended by seven new members. Finally, six chosen steroids were further studied on a preparative scale employing a recombinant *B. megaterium* MS941 whole-cell system, yielding sufficient amounts of product for structure characterization by nuclear magnetic resonance. The hydroxylase activity was confirmed at positons 6β, 7β, 9α, and 15β. In addition, the CYP106A subfamily showed unprecedented 11-oxidase activity, converting 11β-hydroxysteroids to their 11-keto derivatives. This novel

reaction and the diverse hydroxylation positions on pharmaceutically relevant compounds underline the role of the CYP106A subfamily in drug development and production.

Keywords CYP106A1 · CYP106A2 · Cortisol · Cortisone · 11β-Hydroxysteroid dehydrogenation

✉ Rita Bernhardt
ritabern@mx.uni-saarland.de

[1] Institute of Biochemistry, Saarland University, Campus B 2.2, 66123 Saarbruecken, Germany

[2] Institute of Pharmaceutical Biology, Saarland University, 66123 Saarbruecken, Germany

[3] Institute of Bioanalytical Chemistry, Saarland University, 66123 Saarbruecken, Germany

Introduction

For the past decade, cytochrome P450 enzymes (P450s) have been studied as candidates for pharmaceutical drug and drug precursor development. This large superfamily of heme cofactor-containing monooxygenases (http://drnelson.uthsc.edu/CytochromeP450.html) is involved in the catalysis of a wide range of reactions from hydroxylations, epoxidations, and deaminations to dealkylations and C–C bond cleavage. Not only do they perform versatile reactions, they also convert a broad range of substrates. P450s participate in the biosynthesis of endogenous steroids, fatty acids and vitamins as well as in the elimination of exogenous compounds, xenobiotics, and drugs (Bernhardt 2006; Urlacher et al. 2004). They are thus suitable for the production of pharmaceutical compounds and provide a more economically and ecologically sustainable alternative to chemical synthesis, even more so, where the latter has failed to produce sufficient amounts of product (Bernhardt and Urlacher 2014; Urlacher and Girhard 2012). The chemical synthesis of steroids is very complex and costly, particularly when performing regioselective and stereoselective hydroxylations. Microbial/enzymatic transformations are, therefore, favored by the industry as a straightforward, greener, and more cost-effective solution (Donova and Egorova 2012; Tong and Dong 2009).

The heterologous expression of bacterial P450 enzymes was shown to be successful in several host organisms, making the Class I bacterial P450 systems preferable over their membrane-bound mammalian counterparts, due to their solubility and easy handling (Bernhardt 2006; Hannemann et al. 2007; Venkataraman et al. 2014). Although their expression and purification is possible at an analytical scale, the use of isolated P450s in industrial applications is not feasible, mainly due to their instability under process conditions and the need for a constant supply of the rather expensive cofactor NADP(H) (Bernhardt and Urlacher 2014; O'Reilly et al. 2011; Urlacher and Eiben 2006). The latter has been addressed by both enzymatic and chemical methods (Chefson and Auclair 2006; Hollmann et al. 2006), along with the progress toward improved thermostability (Li et al. 2007) and solvent tolerance (Seng Wong et al. 2004). A different possible workaround is the construction of whole-cell systems, where the P450 is expressed by a microbial host organism. These constructs have the advantage of stabilizing the P450 integrity and electron transfer and provide cofactor regeneration by the cellular metabolism. Numerous organisms have been described to realize the heterologous expression of P450s, including the most widely used, *Escherichia coli* (Agematu et al. 2006; Bracco et al. 2013; Makino et al. 2014). Nevertheless, there are cases when using *E. coli* can lead to limitations, such as the restricted transport of large hydrophobic molecules across the cell membrane (Janocha and Bernhardt 2013; Zehentgruber et al. 2010). Another candidate, *Bacillus megaterium*, has recently aroused greater interest as a genetically modified host organism for biotechnological/industrial approaches, especially for the expression of heterologous proteins. On account of having its own P450 expression system, it does not require the addition of the heme-precursor (δ-aminolevulinic acid) in contrast to *E. coli* which lacks natural P450 genes and heme proteins. Its attractive characteristics also include: growth on various carbon sources, high plasmid stability, and no alkaline protease or endotoxin production (Bleif et al. 2012; Korneli et al. 2013; Vary et al. 2007).

From a biotechnological standpoint, CYP106A2 from the *B. megaterium* strain ATCC 13368 (Berg et al. 1976, 1979) and its unique hydroxylating properties raised interest in the past years (Hannemann et al. 2006; Virus and Bernhardt 2008). CYP106A2, being extensively studied since the late 1970s, is a highly active steroid hydroxylase, catalyzing mainly the 15β-hydroxylation of 3-*oxo*-Δ4-steroids (Berg et al. 1976, 1979). Furthermore, the enzyme was shown to hydroxylate diterpenes and triterpenes (Bleif et al. 2011, 2012; Schmitz et al. 2012) and, recently, was also described as a regioselective hydroxylase for the 3-hydroxy-Δ5 steroid dehydroepiandrosterone (Schmitz et al. 2014). Although its original name, 15β-hydroxylase, suggests mainly hydroxylation at the 15β-position, the long-thought strict regioselectivity was contradicted by the identification of 6β, 7α/β, 9α, 11α,

and 15α-hydroxy products (Lisurek et al. 2004, 2008; Nguyen et al. 2012; Virus et al. 2006). Even though these hydroxylations occur in lower proportions, the resulting products are of industrial interest. This means a unique potential for industrial applications, since there is a wide variety of compounds that could serve as substrates for this enzyme. Its natural substrate is yet to be identified, and its substrate range is continuously broadening as a result of library screening (Schmitz et al. 2012, 2014).

The lesser known CYP106A1 shares 63 % amino acid sequence identity and 76 % similarity with its well-studied sibling, CYP106A2 (He et al. 1989, 1995). CYP106A1 from *B. megaterium* DSM319 was recently purified and characterized by our group (Brill et al. 2014) and successfully applied in a whole-cell system for the hydroxylation of a triterpene, 11-keto-β-boswellic acid (KBA), at 7β- and 15α-positions. The CYP106A1-dependent conversion showed a different product pattern compared with CYP106A2 (Bleif et al. 2012), resulting in two additional products, identified as 7β-hydroxy-KBA and 7β,15α-dihydroxy KBA. Furthermore, CYP106A1 was also characterized in vitro from another *B. megaterium* strain, ATCC 14581 by Lee et al. (2014), who recognized some steroids as convertible substrates, but leaving product structures unidentified. Based on the high sequence identity between the two enzymes, CYP106A1 was proposed to be an equally promising candidate in a possible transition of the pharmaceutical industry toward greener processes. In order to exploit the potential of CYP106A1 and to reveal the anticipated differences in activity and selectivity between the two subfamily members, we decided to focus on steroid conversions. Steroids are pharmaceuticals of great importance. Drugs based on the steroid structure are widely used in almost all fields of healthcare, from antimicrobial and antiviral agents to the treatment of hormone-dependent cancer forms (Donova and Egorova 2012). Moreover, steroid hydroxylation is considered to be one of the most important reactions in steroid functionalization, since the derivatives have enhanced biological activity or can be further modified in drug development (Choudhary et al. 2005, 2011, Janeczko et al. 2009).

Here, we tested a focused substrate library with both CYP106A subfamily members and extended their substrate ranges with respect to different steroid molecules. Of the 23 screened steroids, 19 were successfully converted by both enzymes during in vitro and in vivo reactions. Using recombinant *B. megaterium* MS941 whole-cell systems, overexpressing each enzyme, sufficient amounts of product were obtained for structure characterization by nuclear magnetic resonance (NMR). Besides confirming the production of monohydroxylated and dihydroxylated products at 6β-, 7β-, 9α-, and 15β-positions, we were able to demonstrate a previously unknown reaction among these P450s, an 11β-hydroxysteroid dehydrogenase activity. Our recent findings

underline the role of the CYP106A subfamily in the field of drug development and production.

Materials and methods

Reagents and chemicals

All steroid substrates were purchased from Sigma Aldrich Biochemie Gmbh (Germany), all other chemicals were obtained from standard sources and of highest grade available.

Expression and purification of the enzymes

The expression and purification of the CYP106A1 and CYP106A2 proteins was performed as described previously (Brill et al. 2014; Lisurek et al. 2004; Simgen et al. 2000). For the reconstituted in vitro system, a truncated form of bovine adrenodoxin ($Adx_{4–108}$) was used in combination with bovine adrenodoxin reductase (AdR). Their expression and purification was completed as described elsewhere (Sagara et al. 1993; Uhlmann et al. 1992).

UV–visible absorbance spectroscopy

To analyze the characteristics of the purified CYP106A family members, the UV–visible absorbance spectrum of the proteins was recorded in a range of 200–700 nm with a double-beam spectrophotometer (UV-2101 PC, Shimadzu, Japan). The spectra were constantly analyzed during the purification process, approaching a Q value (A_{417}/A_{280}) higher than 1.5, suggesting a high amount of well-folded, heme-containing, and active P450s. The concentration of the proteins for further experiments was determined by CO difference spectroscopy according to the method of Omura and Sato (1964), using an extinction coefficient for the CO-bound P450 of 91 mM^{-1} cm^{-1}.

Substrate binding assay

The substrate binding difference spectra were investigated using a double-beam spectrophotometer (UV-2101PC, Shimadzu, Japan) and tandem quartz cuvettes. The reaction was carried out in 800 μl total volume. One chamber of each cuvette contained 10 μM solution of the enzymes in 50 mM potassium phosphate buffer pH 7.4, while the other chamber was filled with the buffer only. The substrate was dissolved in DMSO at a stock concentration of 20 mM. The enzyme solution was then titrated with increasing concentrations of the substrate. In each step, the same amount of substrate was also added to the buffer-containing chamber of the reference cuvette. After each titration step, the spectrum was recorded between 350 and 500 nm. The K_d value was calculated after the titration of the substrate until saturation. The data was analyzed by plotting the peak-to-through differences against the concentrations of the substrate. The data was fitted in OriginLab Corporations (Massachusetts, USA) using hyperbolic regression. The K_d values are averaged from three independent measurements.

In vitro conversions

The in vitro conversion of the substrates was carried out with a reconstituted system in a final volume of 250 μl at 30 °C for 60 min in 50 mM potassium phosphate buffer (pH 7.4), containing 20 % (v/v) glycerol. The reconstituted system contained AdR (1 μM), the truncated form of bovine $Adx_{4–108}$ (10 μM), CYP106A1 and CYP106A2 (1 μM), an NADPH-regenerating system [MgCl2 (1 mM), glucose-6-phosphate (5 mM), glucose-6-phosphate dehydrogenase (1 U), and NADPH (0.1 μM)], and the substrate (200 μM). The reaction was started by adding NADPH (100 μM) and stopped by the addition of 250 μl of ethyl acetate, mixed vigorously, and extracted twice. After evaporating the combined organic phases to dryness, the residues were dissolved in the high-performance liquid chromatography (HPLC) mobile phase and subjected to HPLC analysis.

In vivo conversions

The in vivo steroid conversions were performed using the recombinant *B. megaterium* MS941 strain, derived from the strain DSM319 (Wittchen and Meinhardt 1995), lacking the major extracellular protease gene *nprM*. The *B. megaterium* MS941 strain was transformed with the corresponding plasmid pSMF2.1B (containing CYP106A1 cloned into *Spe*I/*Mlu*I sites (Brill et al. 2014)) or pSMF2.1C (containing CYP106A2 cloned into *Spe*I/*Mlu*I sites (Bleif et al. 2012)) applying a polyethylene glycol-mediated technique using protoplasts (Barg et al. 2005). To make sure that the conversion was catalyzed by the anticipated enzyme, the conversions were compared to transformations with the wild-type strain MS941 (lacking the pSMF2.1 plasmid, but naturally containing cytochrome P450 genes) as a control. According to these results, the wild-type strain did not show any conversion.

Precultures were inoculated from −80 °C glycerol stock, using 25 ml complex TB medium (24 g l^{-1} yeast extract, 12 g l^{-1} soytone, 2.31 g l^{-1} KH$_2$PO$_4$, and 12.5 g l^{-1} K$_2$HPO$_4$) supplemented with 10 μg ml^{-1} tetracycline and incubated overnight, at 150 rpm, 30 °C. The main culture (supplemented with the corresponding amount of tetracycline) was inoculated with 1 % of the culture volume from the overnight culture. Following the inoculation of the main culture, it was further incubated for 2–3 h, until it reached an OD$_{578}$=0.4 when 0.5 g l^{-1} xylose solution was added to induce the expression. Cells were cultivated for 24 h under the same

conditions prior to the addition of the substrate. For analytical purposes, the experiments were performed in 2 ml reaction tubes with a 500 μl volume of the freshly aliquoted main culture. The transformations required the use of an Eppendorf thermomixer (Eppendorf, Hamburg, Germany) for the continuous mixing with 1,000 rpm, keeping the temperature constant at 30 °C, for 1–4 h. For the preparative scale conversions, 50 ml culture volume was used in 300 ml baffled shake flasks, inoculated with 500 μl of the precultures, induced and cultivated for 24 h at 30 °C, before the addition of the substrates. Conversions at a larger scale were performed with resting cells, either adding the substrate directly 24 h after the expression or after harvesting the cells and suspending them in 100 mM potassium phosphate buffer (pH 7.4). The steroids were added as ethanolic solution to the culture medium (the use of ethanol did not exceed 5 % of the culture volume). Following the corresponding conversion time, the reaction was stopped and the steroids were extracted twice by the addition of 50 ml ethyl acetate. The organic phase was dried over anhydrous $MgSO_4$ and concentrated to dryness in a rotatory evaporator (Büchi R-114). The yellowish residue was dissolved in the mobile phase of the HPLC and filtered through a sterile syringe filter (Rotilabo syringe filter, 0.22 μm, Carl Roth GmbH, Karlsruhe, Germany). The products were separated by preparative HPLC, according to its retention time. The collected fractions were evaporated to dryness and analyzed by NMR spectroscopy and high-resolution mass spectrometry (HRMS).

HPLC analysis

The HPLC analysis was performed on a Jasco system consisting of a Pu-980 HPLC pump, an AS-950 sampler, a UV-975 UV–Vis detector, and an LG-980-02 gradient unit (Jasco, Gross-Umstadt, Germany). A reversed-phase ec MN Nucleodor C_{18} (3 μM, 4.0×125 mm) column (Macherey-Nagel, Betlehem, PA, USA) was used to carry out the experiments, kept at an oven temperature of 40 °C. The steroids were eluted from the column using a gradient method, starting with a mobile phase ratio of 1:9 of $ACN:H_2O$ and increasing it to 1:1. The used flow rate was 1 ml min^{-1}, and the UV detection of the substrate and product was accomplished at 240 or 254 nm. In the case of the isolation of conversion products, the conditions of the preparative reversed-phase HPLC [ec MN Nucleodur C_{18} VP (5 μM, 8×250 mm), Macherey-Nagel, Betlehem, PA, USA] varied according to the size of the column; consequently, the maximum injectable amount of sample could reach 1 ml and the flow rate 2.5 ml min^{-1}.

The conversion and product distribution were calculated from the relative peak area (area %) of the HPLC chromatograms. Following the conversion, all peak areas were summed up and the respective product peak area was divided by the total area of all peaks. The results are presented as conversion % and product formation %.

HRMS analysis

Analyses were performed using a solariX 7 Tesla FTICR mass spectrometer (Bruker Daltonik, Bremen, Germany). All samples were ionized by atmospheric pressure chemical ionization (APCI) in negative ionization mode, using the following parameters: dry temperature 350 °C, vaporizing temperature 350 °C, corona needle 40,000 nA, capillary voltage 2,000 V, end plate offset −500 V, estimated R. P. (400 m/z) 70,000. The calculated exact and measured accurate masses are presented next to each identified compound name in the NMR section.

NMR characterization of the metabolites

The NMR spectra were recorded in $CDCl_3$ or CD_3OD with a Bruker DRX 500 or a Bruker Avance 500 NMR spectrometer at 300 K. The chemical shifts were relative to $CHCl_3$ at δ 7.26 or CH_3OD at δ 3.30 (^{1}H NMR) and $CDCl_3$ at δ 77.00 or CD_3OD at δ 49.00 (^{13}C NMR), respectively, using the standard δ notation in parts per million. The one-dimensional (1D) NMR (^{1}H and ^{13}C NMR, DEPT135) and the two-dimensional (2D) NMR spectra (gs-HH-COSY, gs-NOESY, gs-HSQCED, and gs-HMBC) were recorded using the BRUKER pulse program library. All assignments were based on extensive NMR spectral evidence. (For detailed substrate and product structures, see Table 4.)

6β-Hydroxyandrost-4-ene-3,17-dione

Product A4 (2.6 mg) in the conversion of androstenedione with CYP106A1 (HRMS (APCI) calculated exact mass [Da] $C_{19}H_{26}O_3$ [M+TFA-H]$^-$ 415.1732; measured accurate mass [Da] 415,1733, error [ppm] −0.44). Its ^{1}H NMR data matched those in literature (Kirk et al. 1990). ^{1}H NMR ($CDCl_3$, 500 MHz): δ 0.95 s (3×H-18), 0.98 ddd (12.3, 10.8, and 4.2 Hz, H-9), 1.29 m (H-12a), 1.31 m (H-14), 1.33 m (H-7a), 1.41 s (3×H-19), 1.53 m (H-11a), 1.63 m (H-15a), 1.66 m (6-OH), 1.70 m (H-11b), 1.73 m (H-1a), 1.89 ddd (13.3, 4.2, and 3.0 Hz, H-12b), 1.99 ddd (13.2, 4.0, and 3.0 Hz, H-15b), 2.06 ddd (13.3, 5.0, and 3.0 Hz, H-1b), 2.12 m (H-16a), 2.14 m (H-7b), 2.18 m (H-8), 2.41 m (H-2a), 2.49 m (H-16b), 2.53 m (H-2b), 4.41 ddd (3× 2.5 Hz, H-6), 5.84 brs (H-4). ^{13}C NMR ($CDCl_3$, 125 MHz): δ 13.79 (CH_3, C-18), 19.59 (CH_3, C-19), 20.29 (CH_2, C-11), 21.72 (CH_2, C-15), 29.43 (CH, C-8), 31.30 (CH_2, C-12), 34.20 (CH_2, C-2), 35.76 (CH_2, C-16), 37.13 (CH_2, C-1), 37.22 (CH_2, C-7), 38.05 (C, C-10), 47.63 (C, C-13), 50.93 (CH, C-14), 53.68 (CH, C-9), 72.94 (CH, C-6), 126.64 (CH, C-4), 167.43 (C, C-5), 199.97 (C, C-3), 220.33 (C, C-17).

7β-Hydroxyandrost-4-ene-3,17-dione

Product A2 (3 mg) in the conversion of androstenedione with CYP106A1 {HRMS (APCI) calculated exact mass [Da] $C_{19}H_{26}O_3$ [M+TFA-H]⁻ 415.1732; measured accurate mass [Da] 415,1731, error [ppm] 0.06}. Its ¹H NMR data matched those in literature (Kirk et al. 1990): ¹H NMR (CDCl₃, 500 MHz): δ 0.95 s (3×H-18), 1.01 ddd (12.4, 10.5, and 4.0 Hz, H-9), 1.24 s (3×H-19), 1.26 ddd (2×.3 and 4.2 Hz, H-12a), 1.47 m (H-14), 1.50 m (H-11a), 1.57 m (7-OH), 1.67 ddd (13.5, 13.5, and 5.0 Hz, H-1a), 1.75 m (H-11b), 1.76 ddd (3×10.5 Hz, H-8), 1.88 ddd (13.3, 5.0, and 3.3 Hz, H-12b), 1.94 m (H-15a), 2.06 ddd (13.5, 5.0, and 3.3 Hz, H-1b), 2.13 ddd (19.5 and 2×9.5 Hz, H-16a), 2.32 m (H-15b), 2.39 m (H-2a), 2.45 m (H-2b), 2.48 m (H-16b), 2.49 m (H-6a), 2.58 dd (14.0 and 5.2 Hz, H-6b), 3.59 m (H-7), 5.78 d (2.0 Hz, H-4). ¹³C NMR (CDCl₃, 125 MHz): δ 13.96 (CH₃, C-18), 17.38 (CH₃, C-19), 20.37 (CH₂, C-11), 24.98 (CH₂, C-15), 31.22 (CH₂, C-12), 33.89 (CH₂, C-2), 35.65 (CH₂, C-1), 35.97 (CH₂, C-16), 38.04 (C, C-10), 42.59 (CH, C-8), 42.69 (CH₂, C-6), 48.01 (C, C-13), 50.52 (CH, C-14), 50.78 (CH, C-9), 74.37 (CH, C-7), 125.09 (CH, C-4), 166.35 (C, C-5), 198.95 (C, C-3), 220.39 (C, C-17).

15β-Hydroxyandrost-4-ene-3,17-dione

Product B6 (3.7 mg) in the conversion of androstenedione with CYP106A2 {HRMS (APCI) calculated exact mass [Da] $C_{19}H_{26}O_3$ [M+TFA-H]⁻ 415.1732; measured accurate mass [Da] 415,1752, error [ppm] 4.78}. Its ¹³C NMR data matched those in literature (Mineki et al. 1995) ¹H NMR (CDCl₃, 500 MHz): δ 1.04 ddd (14.8, 10.7, and 4.2 Hz, H-9), 1.22 m (H-7a), 1.23 s (3×H-18), 1.26 s (3×H-19), 1.29 m (H-12a), 1.30 m (H-14), 1.52 m (H-11a), 1.74 m (H-1a), 1.75 m (H-11b), 1.85 ddd (13.2, 4.8, and 3.2 Hz, H-12b), 2.06 m (H-1b), 2.11 m (H-8), 2.15 m (H-7b), 2.36 m (H-2a), 2.37 m (H-6a), 2.43 m (H-2b), 2.50 m (H-6b), 2.52 dd (19.6 and 6.0 Hz, H-16a), 2.59 dd (19.6 and 1.3 Hz, H-16b), 4.59 ddd (6.0, 4.5, and 1.3 Hz, H-15), 5.77 brs (H-4). ¹³C NMR (CDCl₃, 125 MHz): δ 17.26 (CH₃, C-19), 17.59 (CH₃, C-18), 20.26 (CH₂, C-11), 30.47 (CH₂, C-7), 31.44 (CH, C-8), 32.46 (CH₂, C-6), 32.61 (CH₂, C-12), 33.91 (CH₂, C-2), 35.73 (CH₂, C-1), 38.80 (C, C-10), 46.70 (C, C-13), 47.06 (CH₂, C-16), 54.24 (CH, C-9), 54.96 (CH, C-14), 67.16 (CH, C-15), 124.23 (CH, C-4), 170.12 (C, C-5), 199.30 (C, C-3), 219.05 (C, C-17).

7β,15β-Dihydroxyandrost-4-ene-3,17-dione

Product B3 (2 mg) in the conversion of androstenedione with CYP106A2 {HRMS (APCI) calculated exact mass [Da] $C_{19}H_{26}O_4$ [M+TFA-H]⁻ 431.1682; measured accurate mass [Da] 431,1685, error [ppm] 0.81}. The ¹H and ¹³C NMR

spectra showed signals for two secondary hydroxyl groups with similar chemical shifts to those of the monohydroxylated androstenedione derivatives A2 and B6. The positions of the hydroxyl groups at C-7 and C-15 were supported by the results of 2D NMR experiments (HHCOSY, HSQC and HMBC). For example, H-7 ($δ_H$ 3.74 ddd) showed correlations to the H-6a and H-6b (2.58 m, 2H) and H-8 (2.12 ddd) in the HHCOSY, H-15 could be assigned by its vicinal couplings to H-14, H-16a and H-16b in the HHCOSY and its ³J_{CH} correlation with carbonyl C-17 in the HMBC. The β-orientation for both hydroxyls could be concluded by results of the NOESY spectrum. H-7 and H-15 showed an effect to each other and both to the α-orientated H-14; H-7 showed an additional effect to the α-orientated H-9. Therefore, both H-7 and H-15 were in α-position and as a consequence their corresponding hydroxyls β-orientated. To our knowledge, the structure of this dihydroxylated androstenedione has not been reported so far. ¹H NMR (CDCl₃, 500 MHz): δ 1.06 ddd (12.5, 10.7, and 4.2 Hz, H-9), 1.26 s (3×H-18), 1.27 m (H-12a), 1.28 s (3×H-19), 1.40 dd (10.7 and 4.5 Hz, H-14), 1.58 m (H-11a), 1.68 ddd (2×13.5 and 5.0 Hz, H-1a), 1.76 m (H-11b), 1.83 ddd (12.7, 4.0, and 2.5 Hz, H-12b), 2.08 ddd (13.5, 5.0, and 3.3 Hz, H-1b), 2.12 ddd (3×10.7 Hz, H-8), 2.38 m (H-2a), 2.44 m (H-2b), 2.53 dd (20.0 and 8.0 Hz, H-16a), 2.58 m (2H, H-6a, and H-6b), 2.67 dd (20.0 and 1.2 Hz, H-16b), 3.74 ddd (9.5 and 2×8.0 Hz, H-7), 4.66 ddd (7.0, 4.5, and 1.2 Hz, H-15), 5.79 brs (H-4). ¹³C NMR (CDCl₃, 125 MHz): δ 17.34 (CH₃, C-19), 17.65 (CH₃, C-18), 20.38 (CH₂, C-11), 32.16 (CH₂, C-12), 33.86 (CH₂, C-2), 35.58 (CH₂, C-1), 38.01 (C, C-10), 38.56 (CH, C-8), 42.46 (CH₂, C-6), 44.53 (CH₂, C-16), 47.06 (C, C-13), 51.01 (CH, C-9), 55.07 (CH, C-14), 68.52 (CH, C-15), 73.74 (CH, C-7), 125.37 (CH, C-4), 165.67 (C, C-5), 198.90 (C, C-3), 219.50 (C, C-17).

15β-Hydroxycorticosterone

Product D1 (1.2 mg) in the conversion of corticosterone with CYP106A2 {HRMS (APCI) calculated exact mass [Da] $C_{21}H_{30}O_5$ [M-H]⁻ 361.2015; measured accurate mass [Da] 361.2020, error [ppm] 1.27}. Its NMR data showed resonances for an additional hydroxyl group ($δ_C$ 70.24; $δ_H$ 4.41 m), which could be located at position 15β by means of 2D NMR. ¹H NMR (CDCl₃, 500 MHz): δ 1.02 m (H-14), 1.06 m (H-9), 1.15 m (H-7a), 1.19 s (3×H-18), 1.48 s (3×H-19), 1.62 dd (13.8 and 3.3 Hz, H-12a), 1.86 ddd (2×13.5 and 4.5 Hz, H-1a), 2.08 dd (13.8 and 2.8 Hz, H-12b), 2.21 ddd (13.5, 5.0, and 4.0 Hz, H-1b), 2.28 m (2H, H-6a and H-7b), 2.33 m (2H, H-16a and b), 2.34 m (H-17), 2.37 m (H-2a), 2.38 m (H-8), 2.49 m (H-2b), 2.55 m (H-6b), 3.23 dd (2×4.5 Hz, 21-OH), 4.19 dd (18.5 and 4.5 Hz, H-21a), 4.24 dd (18.5 and 4.5 Hz, H-21b), 4.41 m (H-15), 5.70 d (2.0 Hz, H-4). ¹³C NMR (CDCl₃, 125 MHz): δ 18.65 (CH₃, C-18), 20.80 (CH₃, C-19), 27.78 (CH, C-8), 31.70 (CH₂, C-7),

31.82 (CH_2, C-6), 33.79 (CH_2, C-2), 34.78 (C, C-10), 35.04 (CH_2, C-1), 35.53 (CH_2, C-16), 43.46 (C, C-13), 49.13 (CH_2, C-12), 56.64 (CH, C-9), 59.80 (CH, C-17), 61.74 (CH, C-14), 67.80 (CH, C-11), 69.22 (CH_2, C-21), 70.24 (CH, C-15), 122.55 (CH, C-4), 171.36 (C, C-5), 199.32 (C, C-3), 208.77 (C, C-20).

11-Dehydrocorticosterone

Product C5 (2.5 mg) and D4 (1 mg) in the conversion of corticosterone with CYP106A1 and CYP106A2, respectively {HRMS (APCI) calculated exact mass [Da] $C_{21}H_{28}O_4$ [M-H]$^-$ 343.1909; measured accurate mass [Da] 343.1921, error [ppm] 3.34}. The NMR spectra of C5 lacked of resonances for the 11-hydroxy group, but revealed an additional carbonyl (δ_C 207.49) for C-11. ^{1}H NMR (CDCl$_3$, 500 MHz): δ 0.67 s (3× H-18), 1.27 m (H-7a), 1.41 s (3×H-19), 1.45 m (H-15a), 1.63 ddd (2×14.5 and 4.5 Hz, H-1a), 1.80 m (H-14), 1.92 m (2H, H-9, and H-16a), 1.93 m (H-8), 1.95 m (H-15b), 1.98 m (H-7b), 2.29 m (H-16b), 2.30 m (2H, H-2^a, and H-6a), 2.44 m (H-6b), 2.47 d (12.0 Hz, H-12a), 2.48 ddd (17.0, 14.5, and 5.0 Hz, H-2b), 2.56 d (12.0 Hz, H-12b), 2.68 dd (2×9.5 Hz, H-17), 2.77 ddd (14.5, 5.0, and 3.3 Hz, H-1b), 3.16 dd (2×3.5 Hz, 21-OH), 4.14 dd (19.5 and 3.5 Hz, H-21a), 4.19 dd (19.5 and 3.5 Hz, H-21b), 5.73 brs (H-4). ^{13}C NMR (CDCl$_3$, 125 MHz): δ 14.35 (CH_3, C-18), 17.15 (CH_3, C-19), 23.34 (CH_2, C-16), 24.00 (CH_2, C-15), 32.13 (CH_2, C-7), 32.15 (CH_2, C-6), 33.69 (CH_2, C-2), 34.74 (CH_2, C-1), 36.74 (CH, C-8), 38.16 (C, C-10), 47.50 (C, C-13), 54.93 (CH, C-14), 56.20 (CH_2, C-12), 57.56 (CH, C-17), 62.67 (CH, C-9), 69.24 (CH_2, C-21), 124.70 (CH, C-4), 168.03 (C, C-5), 199.53 (C, C-3), 207.49 (C, C-11), 208.98 (C, C-20).

9α-Hydroxy-11-dehydrocorticosterone

Product C2 (1 mg) in the conversion of corticosterone with CYP106A1 {HRMS (APCI) calculated exact mass [Da] $C_{21}H_{28}O_5$ [M-H]$^-$ 359.1859; measured accurate mass [Da] 343.1867, error [ppm] 2.45}. C2 was the only product in our conversion study that formed a tertiary hydroxyl group with the P450 enzymes. Its resonance line at δ_C 79.31 showed $^3J_{CH}$ couplings to H-1a, H-12a, and methyl H-19 in the HMBC spectrum indicating that C-9 bared the additional hydroxyl group. As H-9 in the substrate, 9-OH of the conversion product C2 was α-oriented. This was obvious by the cross-peaks found in NOESY spectrum. Key correlations were found between H-8 and the methyls H-18 and H-19, which therefore must be positioned on the same side of the steroid skeleton. Only two citations from the 50s could be found for the structure of 9α-hydroxy-11-dehydrocorticosterone, but both without NMR data. ^{1}H NMR (CDCl$_3$, 500 MHz): δ 0.66 s (3×H-18), 1.39 m (H-15a), 1.49 s (3×H-19), 1.66 m (H-7a), 1.71 m

(H-7b), 1.82 m (H-15b), 1.94 m (H-16a), 2.10 m (H-1a), 2.17 m (H-8), 2.22 m (H-14), 2.26 m (H-16b), 2.30 ddd (15.0, 4.7, and 2.0 Hz, H-6a), 2.37 m (H-2a), 2.38 d (12.0 Hz, H-12a), 2.47 m (H-2b), 2.48 m (H-6b), 2.50 m (H-1b), 2.73 dd (2×9.5 Hz, H-17), 3.05 dd (12.0 and 1.0 Hz, H-12b), 3.16 dd (2×5.0 Hz, 21-OH), 4.13 dd (19.2 and 4.7 Hz, H-21a), 4.19 dd (19.2 and 4.7 Hz, H-21b), 5.86 d (2.0 Hz, H-4). ^{13}C NMR (CDCl$_3$, 125 MHz): δ 13.91 (CH_3, C-18), 18.89 (CH_3, C-19), 23.32 (CH_2, C-16), 23.72 (CH_2, C-15), 24.52 (CH_2, C-7), 28.15 (CH_2, C-1), 31.29 (CH_2, C-6), 33.74 (CH_2, C-2), 38.65 (CH, C-8), 43.66 (C, C-10), 47.11 (C, C-13), 48.73 (CH, C-14), 51.98 (CH_2, C-12), 57.41 (CH, C-17), 69.28 (CH_2, C-21), 79.31 (C, C-9), 127.68 (CH, C-4), 165.89 (C, C-5), 198.83 (C, C-3), 206.83 (C, C-11), 209.09 (C, C-20).

6β-Hydroxy-11-deoxycorticosterone (6β-hydroxy-DOC)

Product E5 (1.1 mg) in the conversion of 11-deoxycorticosterone with CYP106A1 {HRMS (APCI) calculated exact mass [Da] $C_{21}H_{30}O_4$ [M-H]$^-$ 345.2066; measured accurate mass [Da] 345.2076, error [ppm] 2.82}. Selected ^{1}H NMR data were published by Matsuzaki et al. (1995). Our ^{1}H NMR of E4 matched these data. ^{1}H NMR (CDCl$_3$, 500 MHz): δ 0.73 s (3×H-18), 0.96 ddd (12.5, 11.0, and 4.5 Hz, H-9), 1.17 m (H-14), 1.28 m (H-7a), 1.38 m (H-12a), 1.39 s (3×H-19), 1.40 m (H-15a) 1.49 m (H-11a), 1.63 m (H-11b), 1.73 m (H-1a), 1.77 m (H-16a), 1.79 m (H-15b), 1.97 ddd (12.0, 3.5, and 2.5 Hz, H-12b), 2.01 m (H-8), 2.03 m (H-7b), 2.04 ddd (10.5, 5.0, and 2.8 Hz, H-1b), 2.23 m (H-16b), 2.40 dddd (17.3, 4.5, 3.0, and 1.0 Hz, H-2a), 2.47 brd (9.0 Hz, H-17), 2.49 m (H-16b), 2.53 ddd (17.3, 15.0, and 5.0 Hz, H-2b), 3.25 dd (2×4.5 Hz, far 19-OH), 4.17 dd (19.0 and 4.5 Hz, H-21a), 4.22 dd (19.0 and 4.5 Hz, H-21b), 4.37 dd (2×2.5 Hz, H-6), 5.83 brs (H-4). ^{13}C NMR (CDCl$_3$, 125 MHz): δ 13.50 (CH_3, C-18), 19.53 (CH_3, C-19), 20.87 (CH_2, C-11), 22.91 (CH_2, C-16), 24.43 (CH_2, C-15), 29.74 (CH, C-8), 34.20 (CH_2, C-2), 37.12 (CH_2, C-1), 37.94 (C, C-10), 38.35 (2×CH_2, C-7 and C-12), 44.75 (C, C-13), 53.38 (CH, C-9), 56.06 (CH, C-14), 59.09 (CH, C-17), 69.69 (CH_2, C-21), 73.03 (CH, C-6), 126.51 (CH, C-4), 167.60 (C, C-5), 200.08 (C, C-3), 210.06 (C, C-20).

15β-Hydroxy-11-deoxycorticosterone (15β-hydroxy-DOC)

Product E4 (3.5 mg) and F5 (4 mg) in the conversion of 11-deoxycorticosterone with CYP106A1 and CYP106A2, respectively {HRMS (APCI) calculated exact mass [Da] $C_{21}H_{30}O_4$ [M-H]$^-$ 345.2066; measured accurate mass [Da] 345.2055, error [ppm] −3.06}. In comparison to 11-deoxycorticosterone, the NMR data of E4 and F5 showed signals for an additional secondary hydroxyl group (δ_H 4.38 ddd, δ_C 70.34). Its position at C-15 could be deduced by

vicinal couplings of the methin proton with H-14 (δ_H 1.04) and H-16a (δ_H 2.32) in the HHCOSY and with C-13 (δ_C 44.29) and C-17 (δ_C 59.28) in HMBC. The β-orientation of the hydroxyl was obvious by the NOESY effects of H-15 with H-14 and H-16a, both in α-position. In addition to these results, the chemical shifts of the epimeric 15α-hydroxy-11-deoxycorticosterone (Faramarzi et al. 2003) differed significantly from our values. ^{1}H NMR (CDCl$_3$, 500 MHz): δ 0.96 s (3×H-18), 1.04 m (H-9), 1.06 m (H-14), 1.16 m (H-7a), 1.22 s (3×H-19), 1.38 m (H-12a), 1.43 dddd (3×13.5 and 3.5 Hz, H-11a), 1.66 dddd (13.5 and 3×4.0 Hz, H-11b), 1.73 ddd (2× 13.5 and 5.0 Hz, H-1a), 1.95 m (H-12b), 1.97 m (H-8), 2.05 ddd (13.5, 5.0, and 3.0 Hz, H-1b), 2.14 m (H-7b), 2.32 m (H-16a), 2.33 m (2H, H-6a and H-6b), 2.38 m (H-2a), 2.43 m (2H, H-2b and H-17), 2.49 m (H-16b), 4.18 d (19.0 Hz, H-21a), 4.24 d (19.0 Hz, H-21b), 4.38 ddd (3× 5.5 Hz, H-15), 5.75 brs (H-4). ^{13}C NMR (CDCl$_3$, 125 MHz): δ 15.98 (CH$_3$, C-18), 17.29 (CH$_3$, C-19), 20.84 (CH$_2$, C-11), 31.11 (CH$_2$, C-7), 31.74 (CH, C-8), 32.61 (CH$_2$, C-16), 33.92 (CH$_2$, C-2), 35.78 (CH$_2$, C-1), 36.03 (CH$_2$, C-6), 38.69 (C, C-10), 39.87 (CH$_2$, C-12), 44.29 (C, C-13), 53.94 (CH, C-9), 59.28 (CH, C-17), 60.37 (CH, C-14), 69.39 (CH$_2$, C-21), 70.34 (CH, C-15), 124.09 (CH, C-4), 170.46 (C, C-5), 199.35 (C, C-3), 209.01 (C, C-20).

7β,15β-Dihydroxy-11-deoxycorticosterone (7β, 15β-dihydroxy-DOC)

Product E2 (1.8 mg) and F4 (3 mg) in the conversion of 11-deoxycorticosterone with CYP106A1 and CYP106A2, respectively {HRMS (APCI) calculated exact mass [Da] C$_{21}$H$_{30}$O$_5$ [M-H]$^-$ 361.2015; measured accurate mass [Da] 361.2019, error [ppm] 1.16}. The NMR spectra of E2 and F4 were similar to those of E4, especially for the resonances of C-15 (δ_C 71.55) and H-15 (δ_H 4.50 ddd, 3×5.5 Hz) as well as the coupling pattern of H-15. But E2 bore an additional secondary hydroxyl group with resonances at δ_H 3.62 (ddd, 9.5 and 2×8.0 Hz) and δ_C 74.36. These resonances and the coupling pattern were close to those of the 7β-hydroxy group found for B3. Therefore, the structure of E2 was elucidated as 7β, 15β-dihydroxy-11-deoxycorticosterone, a structure which has not been published so far. 2D NMR measurements supported the structure and led to the full assignments. ^{1}H NMR (CDCl$_3$, 500 MHz): δ 0.99 s (3×H-18), 1.03 m (H-9), 1.12 dd (10.8 and 5.0 Hz, H-14), 1.25 s (3×H-19), 1.33 ddd (2×13.0 and 4.0 Hz, H-12a), 1.50 dddd (3×13.5 and 4.0 Hz, H-11a), 1.67 m (H-1a), 1.68 m (H-11b), 1.95 ddd (13.0, 4.0, and 3.0 Hz, H-12b), 2.05 m (H-8), 2.07 m (H-1b), 2.33 m (2H, H-16a and H-16b), 2.35 m (H-2a), 2.36 m (H-17), 2.41 m (H-2b), 2.55 m (2H, H-6a and H-6b), 3.62 ddd (9.5 and 2× 8.0 Hz, H-7), 4.22 s (2H, H-21a, and H-21b), 4.50 ddd

(3×5.5 Hz, H-15), 5.77 brs (H-4). ^{13}C NMR (CDCl$_3$, 125 MHz): δ 15.63 (CH$_3$, C-18), 17.25 (CH$_3$, C-19), 20.74 (CH$_2$, C-11), 33.54 (CH$_2$, C-16), 33.89 (CH$_2$, C-2), 35.66 (CH$_2$, C-1), 37.95 (C, C-10), 38.52 (CH, C-8), 39.36 (CH$_2$, C-12), 42.60 (CH$_2$, C-6), 44.47 (C, C-13), 50.74 (CH, C-9), 59.01 (CH, C-17), 60.11 (CH, C-14), 69.35 (CH$_2$, C-21), 71.55 (CH, C-15), 74.36 (CH, C-7), 125.10 (CH, C-4), 166.10 (C, C-5), 198.99 (C, C-3), 209.24 (C, C-20).

15β-Hydroxy-11-deoxycortisol (15β-hydroxy-RSS)

Product G4 (5 mg) and H3 (5 mg) in the conversion of RSS with CYP106A1 and CYP106A2, respectively {HRMS (APCI) calculated exact mass [Da] C$_{21}$H$_{30}$O$_5$ [M-H]$^-$ 361.2015; measured accurate mass [Da] 361.2013, error [ppm] 0.72}. Its NMR data showed resonances for an additional hydroxyl group (δ_C 70.29; δ_H 4.31 ddd), which could be located at position 15β by means of 2D NMR. Although 15β-hydroxy-11-deoxycortisol is a known structure NMR data were not available in literature. It should be mentioned that the coupling constants found for H-15α (7.8, 6.0, and 2.3 Hz) differed completely from those found for it in 15β-hydroxy-11-deoxycorticosterone (3×5.5 Hz) and in 15β-hydroxyandrost-4-ene-3,17-dione (6.0, 4.5, and 1.3 Hz). This is caused by the high flexibility of the trans-annulated cyclopentane ring and by the strong influence of the C-17 substitution pattern of its preferred configuration. ^{1}H NMR (CD$_3$OD, 500 MHz): δ 0.89 s (3×H-18), 1.04 ddd (12.3, 10.8, and 4.0 Hz, H-9), 1.13 dddd (13.8, 12.5, 11.5, and 4.0 Hz, H-7a), 1.25 s (3×H-19), 1.41 ddd (12.5, 4.0, and 2.8 Hz, H-12a), 1.48 ddd (2×13.5 and 4.0 Hz, H-11a), 1.67 m (H-11b), 1.71 m (H-1a), 1.72 dd (11.5 and 6.0 Hz, H-14), 1.86 ddd (2×12.5 and 4.0 Hz, H-12b), 2.03 ddd (2× 11.2 and 3.2 Hz, H-8), 2.06 dd (15.5 and 7.5 Hz, H-16a), 2.10 ddd (13.5, 5.2, and 3.0 Hz, H-1b), 2.20 dddd (12.5, 5.7 and 2× 2.8 Hz, H-7b), 2.30 m (H-2a), 2.32 m (H-6a), 2.48 ddd (17.0, 15.0, and 5.3 Hz, H-2b), 2.53 dddd (2×15, 5.5 and 1.7 Hz, H-6b), 2.73 dd (15.5 and 2.3 Hz, H-16b), 4.27 d (19.2 Hz, H-21a), 4.31 ddd (7.8, 6.0, and 2.3 Hz, H-15), 4.62 d (19.2 Hz, H-21b), 5.72 brs (H-4). ^{13}C NMR (CD$_3$OD, 125 MHz): δ 17.63 (CH$_3$, C-19), 18.04 (CH$_3$, C-18), 21.68 (CH$_2$, C-11), 32.66 (CH$_2$, C-7), 32.72 (CH$_2$, C-12), 32.94 (CH, C-8), 33.90 (CH$_2$, C-6), 34.73 (CH$_2$, C-2), 36.81 (CH$_2$, C-1), 40.16 (C, C-10), 47.54 (CH$_2$, C-16), 48.40 (C, C-13), 55.32 (CH, C-9), 55.73 (CH, C-14), 67.70 (CH$_2$, C-21), 70.29 (CH, C-15), 90.27 (C, C-17), 124.17 (CH, C-4), 175.17 (C, C-5), 202.35 (C, C-3), 212.64 (C, C-20).

7β,15β-Dihydroxy-11-deoxycortisol (7β,15β-dihydroxy-RSS)

Product G1 (3.5 mg) in the conversion of RSS with CYP106A1 {HRMS (APCI) calculated exact mass [Da]

$C_{21}H_{30}O_6$ [M-H]$^-$ 377.1964; measured accurate mass [Da] 377.1976, error [ppm] 3.01}. Its ^1H and ^{13}C NMR spectra revealed two additional secondary hydroxyl groups. One of them (δ_C 71.26; δ_H 4.56 ddd, 8.0, 5.6, and 2.6 Hz) gave similar values as found for the 15β-hydroxy group in H3. The other one (δ_C 74.67; δ_H 3.68 ddd, 2×10.0 and 6.5 Hz) showed vicinal couplings to the isochronic protons of H-6 (δ_H 2.56 m, 2H) and to H-8 (δ_H 2.06 m) in the HHCOSY. NOESY cross-peaks between H-7 and the α-oriented H-9, H-14, and H-15 revealed the stereochemistry at C-7 with the hydroxy group in β-orientation. The structure of 7β, 15β-dihydroxy-11-deoxycortisol has not been published so far. ^1H NMR (CDCl$_3$, 500 MHz): δ 1.03 s (3×H-18), 1.06 ddd (2×12.0 and 3.7 Hz, H-9), 1.26 s (3×H-19), 1.39 m (H-12a), 1.48 m (H-11a), 1.67 m (H-1a), 1.70 m (H-12b), 1.72 m (H-11b), 1.77 dd (11.0 and 5.5 Hz, H-14), 2.06 m (H-8), 2.07 m (H-1b), 2.22 dd (15.5 and 8.0 Hz, H-16a), 2.40 m (H-2a), 2.45 m (H-2b), 2.56 m (2H, H-6a and H-6b), 2.63 dd (15.5 and 2.5 Hz, H-16b), 3.68 ddd (2×10.0 and 6.5 Hz, H-7), 4.36 d (19.8 Hz, H-21a), 4.56 ddd (8.0, 5.6, and 2.6 Hz, H-15), 4.70 d (19.8 Hz, H-21b), 5.77 brs (H-4). ^{13}C NMR (CDCl$_3$, 125 MHz): δ 17.28 (CH$_3$, C-19), 17.62 (CH$_3$, C-18), 20.19 (CH$_2$, C-11), 30.22 (CH$_2$, C-12), 33.90 (CH$_2$, C-2), 35.65 (CH$_2$, C-1), 37.95 (C, C-10), 38.25 (CH, C-8), 42.65 (CH$_2$, C-6), 43.25 (CH$_2$, C-16), 48.70 (C, C-13), 50.33 (CH, C-9), 53.96 (CH, C-14), 67.71 (CH$_2$, C-21), 71.26 (CH, C-15), 74.67 (CH, C-7), 87.65 (C, C-17), 125.19 (CH, C-4), 165.99 (C, C-5), 198.98 (C, C-3), 212.29 (C, C-20).

Cortisone

Product I6 (1 mg) in the conversion of cortisol with CYP106A1 {HRMS (APCI) calculated exact mass [Da] $C_{21}H_{28}O_5$ [M-H]$^-$ 359.1858; measured accurate mass [Da] 359.1842, error [ppm] −4.62}. Its ^1H NMR data matched those in literature (Kirk et al. 1990). ^1H NMR (CD$_3$OD, 500 MHz): δ 0.60 s (3×H-18), 1.33 m (H-7a), 1.42 s (3×H-19), 1.46 m (H-15a), 1.70 m (H-16a), 1.72 m (H-1a), 1.92 m (H-15b), 2.01 m (H-8), 2.02 m (H-7b), 2.04 d (12.5 Hz, H-12a), 2.11 d (10.5 Hz, H-9), 2.23 ddd (17.0 and 2× 3.8 Hz, H-2a), 2.33 ddd (15.0, 4.0, and 2.5 Hz, H-6a), 2.45 m (H-14), 2.50 m (H-2b), 2.52 m (H-6b), 2.70 m (H-1b), 2.72 m (H-16b), 2.95 d (12.5 Hz, H-12b), 4.22 d (19.5 Hz, H-21a), 4.60 d (19.5 Hz, H-21b), 5.71 brs (H-4). ^{13}C NMR (CD$_3$OD, 125 MHz): δ 16.15 (CH$_3$, C-18), 17.58 (CH$_3$, C-19), 24.14 (CH$_2$, C-15), 33.43 (CH$_2$, C-6), 33.58 (CH$_2$, C-7), 34.44 (CH$_2$, C-2), 35.23 (CH$_2$, C-16), 35.62 (CH$_2$, C-1), 37.88 (CH, C-8), 39.60 (C, C-10), 50.98 (CH, C-14), 51.45 (CH$_2$, C-12), 52.24 (C, C-13), 63.47 (CH, C-9), 67.88 (CH$_2$, C-21), 89.35 (C, C-17), 124.76 (CH, C-4), 172.87 (C, C-5), 202.45 (C, C-3), 212.01 (C, C-11), 212.78 (C, C-20).

6β-Hydroxycortisone

The only under in vivo conditions observed product (2 mg) downstream K1 in the conversion of cortisone with CYP106A1 {HRMS (APCI) calculated exact mass [Da] $C_{21}H_{28}O_6$ [M-H]$^-$ 375.1808; measured accurate mass [Da] 375.1792, error [ppm] −4.22}. Comparison of its ^1H and ^{13}C NMR data with those of the 6β-hydroxy derivatives, A4 and E5 showed striking similarities especially for the hydroxyl moiety. The results of 2D NMR analysis supported the structure. ^1H NMR (CDCl$_3$, 500 MHz): δ 0.69 s (3×H-18), 1.26 m (H-16a), 1.53 m (H-7a), 1.57 m (H-15a), 1.60 s (3×H-19), 1.64 m (H-1a), 1.88 m (H-9), 2.03 m (H-15b), 2.14 m (H-12a), 2.15 m (H-7b), 2.32 m (H-16b), 2.36 m (H-2a), 2.38 m (H-14), 2.42 m (H-8), 2.57 ddd (17.5, 15.0, and 5.0 Hz, H-2b), 2.81 m (H-12b), 2.82 m (H-1b), 4.29 d (19.8 Hz, H-21a), 4.38 dd (2×3.0 Hz, H-6), 4.65 d (19.8 Hz, H-21b), 5.83 brs (H-4). ^{13}C NMR (CDCl$_3$, 125 MHz): δ 16.00 (CH$_3$, C-18), 19.15 (CH$_3$, C-19), 23.42 (CH$_2$, C-15), 30.62 (CH, C-8), 32.06 (CH$_2$, C-16), 34.04 (CH$_2$, C-2), 35.98 (CH$_2$, C-1), 37.81 (C, C-10), 38.91 (CH$_2$, C-7), 49.37 (CH, C-14), 49.76 (CH$_2$, C-12), 51.68 (C, C-13), 62.17 (CH, C-9), 67.54 (CH$_2$, C-21), 72.41 (CH, C-6), 88.06 (C, C-17), 127.20 (CH, C-4), 166.06 (C, C-5), 199.94 (C, C-3), 208.47 (C, C-11), 211.53 (C, C-20).

15β-Hydroxycortisone

Product K3 and L3 (1 mg) in the conversion of cortisone with CYP106A1 and with CYP106A2, respectively {HRMS (APCI) calculated exact mass [Da] $C_{21}H_{28}O_6$ [M-H]$^-$ 375.1808; measured accurate mass [Da] 375.1822, error [ppm] 3.87}. Due to the low amount, only a ^1H NMR and a HHCOSY could be recorded for the samples, indicating an additional secondary hydroxyl group for the conversion product. Comparison of the chemical shift and the coupling pattern of the CHOH resonance (4.62 dd, 7.5, 5.5, and 2.0 Hz) with those of all the other conversion products led to the structure of 15β-hydroxycortisone. ^1H NMR (CDCl$_3$, 500 MHz): δ 0.67 s (3×H-18) 1.47 s (3×H-19), 4.33 d (19.8 Hz, H-21a), 4.62 ddd (7.5, 5.5, and 2.0 Hz, H-15), 4.77 d (19.8 Hz, H-21b), 5.77 brs (H-4).

Results

Expression, purification, and spectral characterization of the proteins

The proteins were expressed and purified (to homogeneity) using a recombinant *E. coli* C43 (DE3) strain. The UV–Vis spectra of both proteins showed characteristic absorbance peaks at 356, 417, 534, and 567 nm in the oxidized form. In

the carbon monoxide-bound reduced form, a peak at 450 nm was clearly observed without a visible peak at 420 nm suggesting no inactive P450 form (Schenkman and Jansson 1998; Fig. S1).

Substrate binding

To compare the steroid hydroxylating capacity of the CYP106A subfamily members, a focused library of 23 steroids was screened for high-spin shift induction using difference spectroscopy (Table 1). The study was performed using difference spectroscopy due to its higher sensitivity, since the extent of the obtained shifts was very small, in all cases less than 10 %. The library included 14 compounds formerly tested with CYP106A2 and nine additional 3-*oxo*-steroids, derivatives of already known substrates of CYP106A2. P450 substrates usually induce a shift of the heme iron to the high-spin state, resulting in a so-called type I shift spectrum (Schenkman et al. 1981). It is known that type I shift-inducing compounds are converted more often than those which do not induce a high spin shift. However, it has been shown previously that even compounds which do not induce a clear type I shift can be converted by P450s (Ferrero et al. 2012; Girhard et al. 2010; Schmitz et al. 2014; Simgen et al. 2000), yet induction of a type I shift does not necessarily lead to product formation (Khatri et al. 2013; Schmitz et al. 2012). In our case, there are two examples listed in Table 1, where type I shift-inducing compounds were not converted (adrenosterone, 19-hydroxyandrostenedione), while successful conversion was observed with pregnenolone and 17-hydroxypregnenolone inducing no shift. The type I binding assay allows us a straight forward comparison of the binding behavior of CYP106A1 and CYP106A2. Only four steroids, β-estradiol, estrone, pregnenolone, and 17β-hydroxypregnenolone, did not induce any spin-shift alteration in CYP106A1 and CYP106A2. There was only one steroid, 19-nortestosterone, which, despite being converted by both enzymes, did not induce any spectral shift with CYP106A2, but induced a type I shift with CYP106A1. Out of 23 steroids tested, 18 showed a clear type I shift induction by both enzymes and product formation was observed with all but four steroids (Table 1). As expected, the two CYP106A family members show similar steroid binding behavior according to spin-state alterations, caused by the displacement of the water molecule as sixth heme iron ligand.

Catalytic activity and dissociation constants

The catalytic activity of the CYP106A subfamily was compared with respect to all 23 steroids (Table 1). Most of the steroids contained the 3-*oxo*-Δ4 moiety, others possessed 3-*oxo*-Δ2,4 or 3-hydroxy-Δ5 structures. Following the HPLC analysis, 19 out of 23 steroids, except 19-hydroxyandrostenedione, adrenosterone, β-estradiol and estrone, were observed to be converted by both subfamily members, with detectable conversion products. Though all 19 steroids were converted both by CYP106A1 and CYP106A2, differences in the product pattern and/or activity were observed when studying 3-*oxo*-Δ4-steroids (Table 2). There was no clear correlation found between the steroid structures, the differences in conversion velocity or side product formation.

However, testing C18-, C19-, C20-, or C21-steroids, CYP106A2 seemed in all cases to be more selective than CYP106A1, showing one or two main products. In most cases, CYP106A1 produced the same main product, but a higher number of side-products. CYP106A2 also showed slightly higher conversion velocity in all transformations except for 11β-hydroxysteroids.

To get deeper insight into the structural basis for the activity and selectivity of steroid hydroxylation, the substrates were narrowed down to six 3-*oxo*-Δ4 steroids (Table 4) whose conversion showed significant differences between CYP106A1 and CYP106A2, either in product pattern or enzyme activity. Since the main product of CYP106A2 was already identified for some of these substrates (Table 1), the recognized differences in the product pattern produced by CYP106A1 suggested hidden potentials in terms of novel products. The dissociation constant of these steroids and their in vitro and in vivo conversion with the resulting product(s) was therefore further investigated.

The binding of the six substrates induced a type I shift with both CYP106A enzymes (Table 1). The equilibrium dissociation constants were determined to investigate the binding affinities toward both enzymes (Table 3), each of which was titrated with increasing concentrations of the corresponding substrates. Saturation of binding was observed in all cases and the binding constants were estimated by hyperbolic regression. In Fig. S2, the binding curves of three substrates tested in this study (corticosterone, cortisol, and cortisone to CYP106A1 and CYP106A2) are shown as an example. Interestingly, both enzymes bind the six steroids with similar affinities, with dissociation constants ranging from 50 μM for 11-deoxycorticosterone (DOC) to 543 μM for cortisol (CYP106A2) and from 68 μM for DOC to 464 μM for cortisone (CYP106A1). The binding affinities of corticosterone, cortisone, and cortisol showed the highest differences, being 2.5-folds and 1.7-folds higher for corticosterone and cortisone, respectively, with CYP106A1 compared with CYP106A2, whereas for cortisol the K_d value was 0.6-fold lower with CYP106A1 than with CYP106A2. The binding affinities are in the higher micromolar range with both enzymes, except for androstenedione and DOC.

Table 1 Overview of the 23 tested steroids concerning their binding and conversion with CYP106A1 and CYP106A2

Steroid	In vitro conversion		Known product formation by CYP106A2	Induction of high spin shift	
	CYP106A1	CYP106A2		CYP106A1	CYP106A2
Testosterone	+	+	15β[a]	+	+
17α-Methyltestosterone	+	+	n.d.	+	+
19-Nortestosterone	+	+	n.d.	+	−
Ethisterone	+	+	n.d.	+	+
Progesterone	+	+	15β[a] (11α, 6β, 9α)	+	+
17α-Hydroxyrogesterone	+	+	15β[a]	+	+
Androstenedione	+	+	15β[a]	+	+
11-Deoxycorticosterone (DOC)	+	+	15β[a]	+	+
11-Deoxycortisol (RSS)	+	+	n.d.	+	+
Corticosterone	+	+	15β[a]	+	+
Cortisol	+	+	n.d.	+	+
Cortisone	+	+	n.d.	+	+
Prednisolone	+	+	n.d.	+	+
Prednisone	+	+	n.d.	+	+
Dexamethasone	+	+	n.d.	+	+
11β-Hydroxyandrostenedione	+	+	n.d.	+	+
19-Hydroxyandrostenedione	−	−	−	+	+
Adrenosterone	−	−	−	+	+
β-Estradiol	−	−	−	−	−
Estrone	−	−	−	−	−
Pregnenolone	+	+	7β[b]	−	−
17α-Hydroxypregnenolone	+	+	7β (7α)[b]	−	−
Dehydroepiandrosterone	+	+	7β (7α)[b]	+	+

+/− positive and negative outcomes of what is stated in the column headers, respectively, *n.d.* hydroxylation position not determined

[a] Berg et al. (1976)

[b] Schmitz et al. (2014)

In vitro conversions

To shed more light on the differences in the hydroxylation pattern of both CYP106A subfamily members, the in vitro conversion of the six chosen steroids was further investigated and the main and some minor conversion products were identified. In order to compare both enzymes with one another and with previously published results, the redox system from bovine adrenals, known to be an efficient electron supplier for bacterial P450s, especially for CYP106A2 (Ewen et al. 2012; Virus et al. 2006), was

used in this work as described elsewhere (Bleif et al. 2012; Schmitz et al. 2012).

Androstenedione was successfully converted by both enzymes, but with different velocities. Using equal enzyme concentrations, after 30 min CYP106A2 converted nearly 100 % of the substrate, producing two main products, B3 and B6, as well as several side products (Fig. 1b). In contrast, CYP106A1 could reach a maximal 84 % total conversion after 60 min (Fig. 1a). Consequently, the activity of CYP106A1 was considered to be lower toward androstenedione, though it also formed two main products, A2 and A4, besides a few minor

Table 2 Summary of the in vitro substrate conversion of steroid compounds with the CYP106A subfamily members

Steroids	Conversion with CYP106A1 and CYP106A2
3-*oxo*-Δ⁴ steroids	Conversion, similar or same product pattern and activity with exceptions (generally more side-product formation for CYP106A1)
3-*oxo*-Δ²,⁴ steroids	Conversion, same product pattern
3-Hydroxy-Δ⁵ steroids	Conversion, same product pattern
Other steroids	No conversion (19-hydroxyandrostenedione, adrenosterone, β-estradiol, and estrone)

Table 3 Overview of the substrate binding to CYP106A1 and CYP106A2 showing the respective K_d values ($R^2 \geq 0.98$ in all cases)

Steroid	K_d value [μM]	
	CYP106A1	CYP106A2
Androstenedione	77 ± 2[a]	81 ± 10[b]
Corticosterone	471 ± 14[c]	185 ± 8[c]
11-Deoxycorticosterone (DOC)	68 ± 2[a]	50 ± 1[c]
11-Deoxycortisol (RSS)	161 ± 5[a]	102 ± 4[c]
Cortisol	307 ± 19[c]	543 ± 31[c]
Cortisone	464 ± 8[c]	260 ± 7[c]

[a] Brill (2013)

[b] Schmitz et al. (2014)

[c] Tested in this work

metabolites. A2, A4, and A6 showed very similar retention times as the CYP106A2's products, B3, B6, and B7, respectively. The minor products A2 and B3 had shorter retention times, thus higher hydrophobicity.

Within 30 min, CYP106A1 converted 41 % of corticosterone into one main product (C5) with low amounts of minor product formation (C1-C4). No significant increase in conversion was observed with longer incubation times (Fig. 1c). The conversion with CYP106A2 resulted in a rather different product pattern. After 30 min, CYP106A2 converted 47 % of the substrate mainly to D1 and D2, whose peaks increased over time, resulting in 57 % conversion within 60 min (Fig. 1d). The CYP106A1 main and minor products (except for C1) showed matching retention times with the CYP106A2 metabolites.

The activity of the CYP106A subfamily members was considered to be similar toward DOC, since they both converted 100 % of the substrate within 60 min to one main (E4, F5) and several minor products (Fig. 1e, f). The main product (E4, F5) of both enzymes, as well as the minor products (E2, F4), had identical retention times. In addition, the minor product ratios increased from 30 to 60 min of conversion, along with the decrease of the main product peak, hence these products were thought to be further oxidized derivatives of the main product.

CYP106A2 showed complete conversion of 11-deoxycortisol (RSS) into one main (H3) and four minor products (H1-H5), already within 30 min (Fig. 1h). CYP106A1 showed similar activity toward the substrate with lower conversion rate and produced a main product (G4) with the same retention time as the CYP106A2 main product (H3) (Fig. 1g). Both enzymes showed side product formation of which G1 and H2 also had identical retention times.

After 4 h, CYP106A1 transformed 77 % of cortisol, while CYP106A2 converted only 55 %. Therefore, the activity of CYP106A2 was considered to be lower toward cortisol. CYP106A1 produced two main products, I5 downstream

and I6 upstream the substrate peak and four side products (I1–I4) (Fig. 1i). Interestingly, using CYP106A1, only the ratio of I3, I4, and I5 increased, while the amounts of the substrate and I6 simultaneously decreased over time. According to the used reversed-phase HPLC system, I6 was believed to be more hydrophobic than the substrate (Fig. 1i). Cortisol conversion with CYP106A2 produced somewhat different results. After 1 h, cortisol was converted into J1 and J3 with low amounts of J2 and J4. The amount of J1 and J3 increased throughout the substrate conversion, showing again more hydrophobic side-product formation (Fig. 1j). The CYP106A1 products I2, I5, and I6 showed exactly the same retention times as J1, J3, and J4 from CYP106A2, suggesting identical structures.

When studying the conversion of cortisone, 93 % of the substrate was converted by CYP106A2 within 1 h, while CYP106A1 showed significantly lower activity with 58 % conversion and reaching only 76 % during the 4 h reaction time (Fig. 1k, l). Besides the difference in their activities, both subfamily members produced one main product (K3 and L3) with the same retention time and two to three minor side products. Interestingly, the main products, K3 and L3, had matching retention times not only with each other but also with I5 and J3 from the cortisol conversion (Fig. 1i, j).

In vivo whole-cell conversions and product identification

Following the comparison of the in vitro activities of both enzymes, which revealed some differences in the product pattern, we aimed to identify the main products via NMR spectroscopy. For this, 200 μM final concentration of the substrate was added to *B. megaterium* resting cells overexpressing the corresponding P450, 24 h after induction. Samples were taken at 1, 2, 4, 8, and 24 h to follow the main and side product formations over time for the final isolation of the main products. Compared with the in vitro results, the product pattern slightly differed using the whole-cell catalyst (Fig. S3). However, the main products remained present in all cases. The novel peaks observed in the in vivo system are most likely further metabolized intermediate products by enzymes naturally present in the strain or remaining traces of the cultivation medium. For this reason, we decided to purify the corresponding main products and some of the minor products already identified during the in vitro experiments. To avoid confusion, the products seen in vitro (Fig. 1) were labeled the same fashion as on the in vivo HPLC chromatograms (Fig. S3). The structures of all six substrates and their identified conversion products are summarized in Table 4.

In vivo, CYP106A1 showed a lower conversion rate with androstenedione compared with CYP106A2, consistent with the in vitro observations. However, both enzymes reached 100 % substrate consumption after 24 h (data not shown). CYP106A1 showed the same product distribution after 4 h
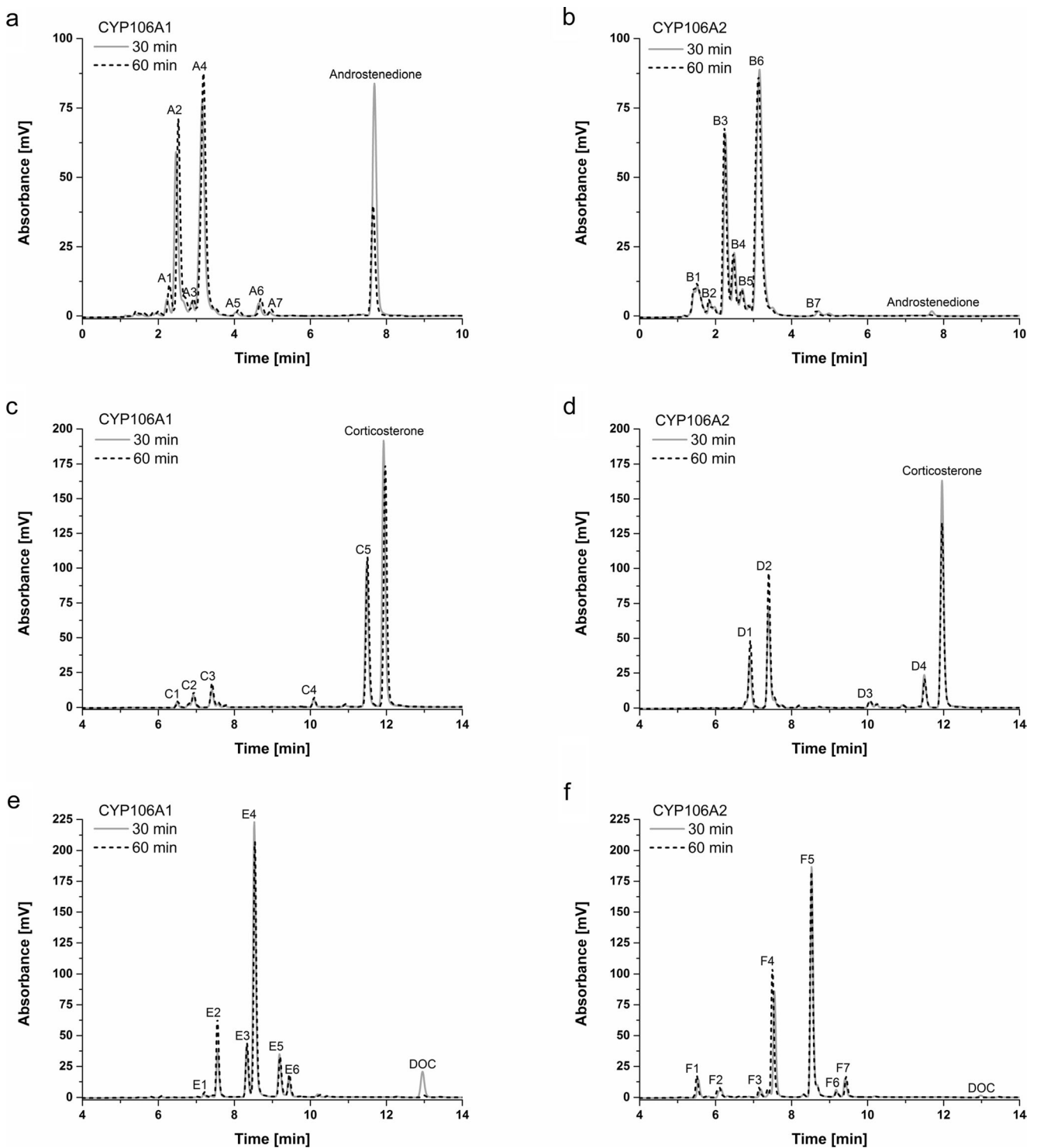
Fig. 1 HPLC chromatograms of the in vitro conversion of androstenedione (**a**, **b**), corticosterone (**c**, **d**), 11-deoxycorticosterone (**e**, **f**), 11-deoxycortisol (**g**, **h**), cortisol (**i**, **j**) and cortisone (**k**, **l**) by CYP106A1 and CYP106A2, respectively. The reaction was performed in 50 mM potassium-phosphate buffer containing 20 % glycerol at 30 °C, using 1 μM AdR, 10 μM Adx$_{4–108}$, and 0.5 μM CYP106A enzymes

(Fig. S3a) as in vitro (Fig. 1a), while CYP106A2 showed a slightly altered one (Fig. S3b). The main metabolite of androstenedione by CYP106A2 was identified as 15β-hydroxyandrostenedione (B6), confirming the results by Berg

et al. (1976). After 8 h, a significant increase in the minor product B3 formation was observed (Fig. S3b), identified as 7β, 15β-dihydroxyandrostenedione. Interestingly, CYP106A1 did not show 15β-hydroxylase activity toward
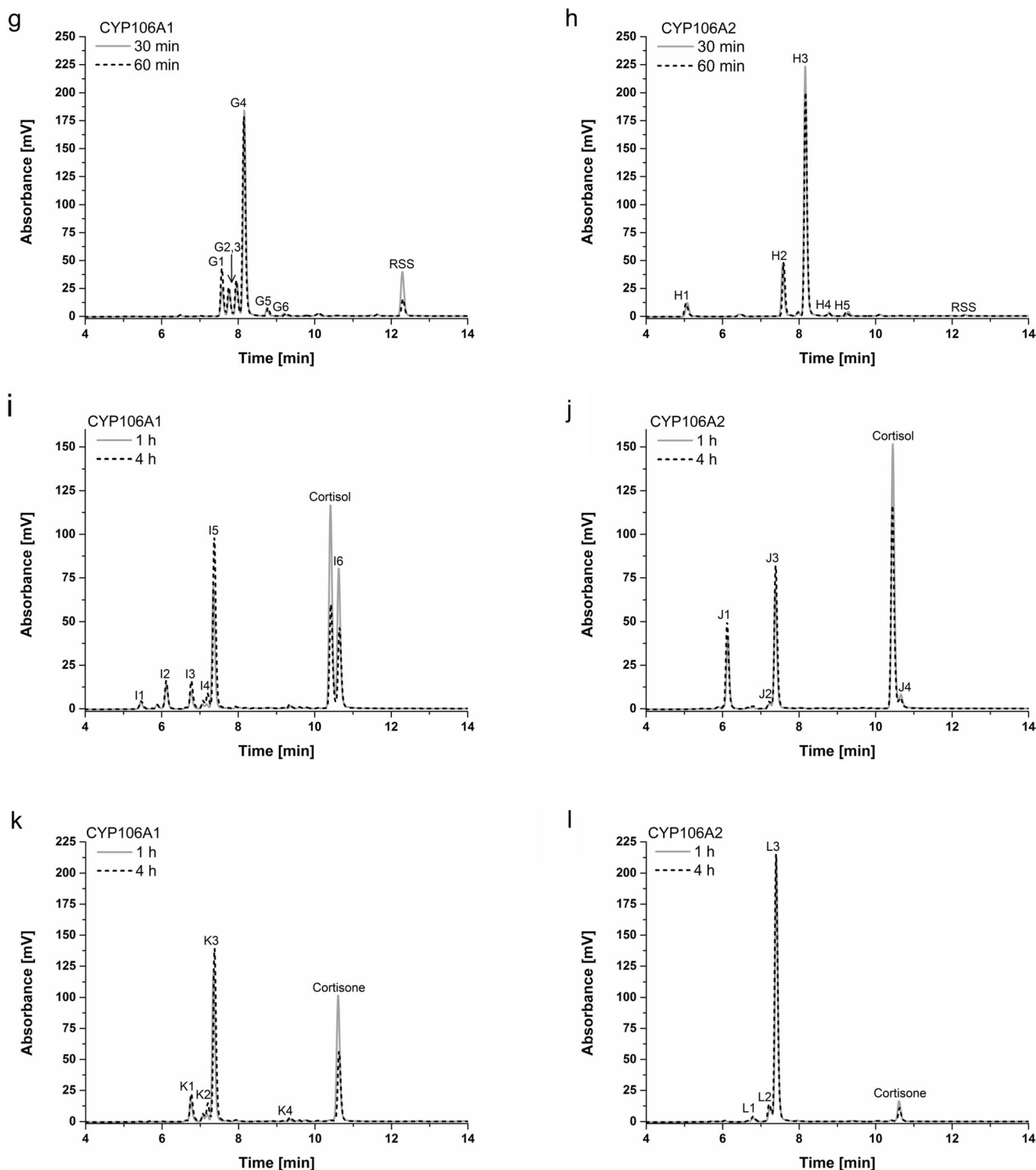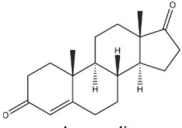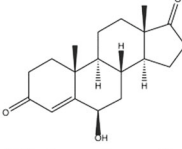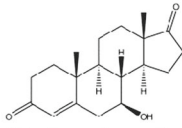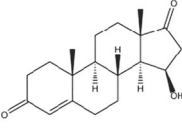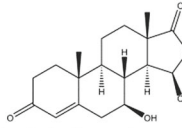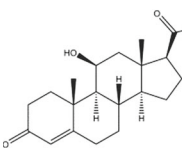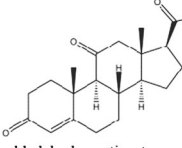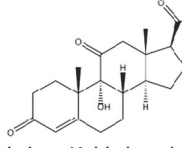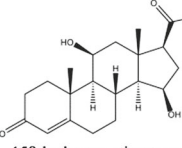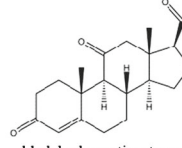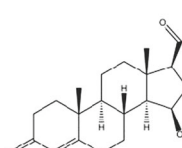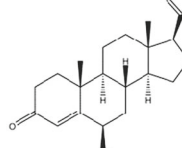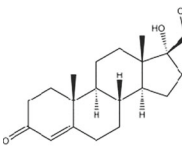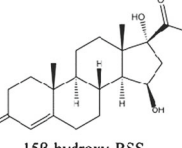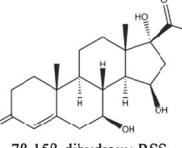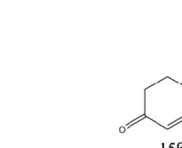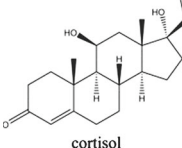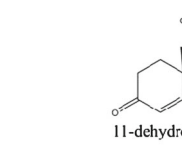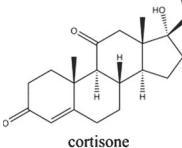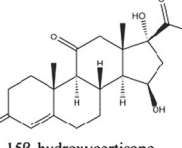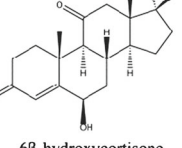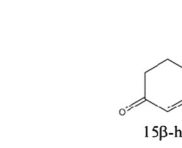
Fig. 1 (continued)

its novel substrate. It produced the pharmaceutically promising 6β-hydroxyandrostenedione and 7β-hydroxyandrostenedione (A4 and A2, respectively) as main metabolites, highlighting the difference in selectivity between the two subfamily members (Fig. S3a).

CYP106A1 applied in the whole-cell system showed 89 % conversion of corticosterone in 8 h compared with a maximum 45 % product formation in vitro. The product pattern within 4 h was similar to the one seen in vitro, showing C5 as main product. However, after 8 h, it shifted toward the minor

Table 4 Overview of the six studied steroids, including their conversion products by the CYP106A1 and CYP106A2 enzymes. (The product distribution is given in % after 4 h of conversion, if not otherwise indicated.)

Converted steroids	Identified conversion products			
	CYP106A1		CYP106A2	
androstenedione	6β-hydroxyandrostenedione (31 %)	7β-hydroxyandrostenedione (22 %)	15β-hydroxyandrostenedione * (67 %)	7β,15β-dihydroxyandrostenedione (9 %)
corticosterone	11-dehydrocorticosterone (38 %)	9α-hydroxy-11-dehydrocorticosterone (4 %)	15β-hydroxycorticosterone * (16 % in 4h, 26 % in 8h)	11-dehydrocorticosterone (7 % in 4h, 5 % in 8h)
11-deoxycorticosterone (DOC)	15β-hydroxy-DOC (28 %) / 6β-hydroxy-DOC (9 %) / 7β,15β-dihydroxy-DOC (37 %)		15β-hydroxy-DOC * (66 %)	7β,15β-dihydroxy-DOC (21%)
11-deoxycortisol (RSS)	15β-hydroxy-RSS (36 % in 1h, 9 % in 4h)	7β,15β-dihydroxy-RSS (8 % in 1h, 18 % in 4h)	15β-hydroxy-RSS (76 % in 1h, 33 % in 4h)	
cortisol	11-dehydrocortisol (cortisone) (19 %)		n.d.	
cortisone	15β-hydroxycortisone (14 %)	6β-hydroxycortisone (6 %)	15β-hydroxycortisone (40 %)	

* Also identified by Berg et al. (1976)

n.d. product structure not determined

products (C1–C4; Fig. S3c). CYP106A2 converted 56 % of the substrate within 8 h under in vivo conditions, comparable to the in vitro conversion. The product distribution was similar as seen before, with D1 and D2 as main products and a small

amount of D4 formation. An additional product peak was also observed downstream D1, having the same retention time as C1 (Fig. S3d). The main products of CYP106A1 (C5) with matching retention time to the minor metabolite of CYP106A2 (D4) were both identified as 11-dehydrocorticosterone, justifying the assumption of Lee et al. (2014), that a dehydrogenation takes place during the corticosterone conversion. This is the first case where an 11β-hydroxysteroid dehydrogenation is observed, an unexampled transformation by the CYP106A subfamily. In addition, the main metabolite of CYP106A2 (D1) was characterized as the 15β-hydroxylated derivative, matching the results of Berg et al. (1976). The minor metabolite of CYP106A1 was also successfully characterized as 9α-hydroxy-11-dehydrocorticosterone (C2).

Both CYP106A enzymes showed high activity toward DOC, with complete conversion within 2 h (Fig. S3e, f) and the same product pattern as seen in vitro (Fig. 1e, f). The NMR characterization of the CYP106A1 main product exposed the 15β-hydroxy derivative (E4) just like in the case of CYP106A2 (F5) which was formerly identified by Berg et al. (1976). CYP106A1 showed 6β-hydroxy metabolite formation as well (E5), demonstrating again a stronger affinity for B-ring oxidations compared to CYP106A2. The latter also produced a metabolite (F6) with the same retention time as the 6β-hydroxy-DOC, but in significantly minor amounts. The minor metabolites, E2 and F4, increased over time, while the 15β-hydroxy-DOC decreased, indicating further hydroxylation of the main metabolite (Fig. S3e, f). These minor products (E2, F4) were successfully purified and identified as 7β, 15β-dihydroxy-DOC.

In vivo, the CYP106A enzymes displayed similarly high activity to RSS, both completing the conversion after 4 h. Within the first hour of conversion both enzymes displayed similar product distribution as observed in vitro. G4 and H3 were identified as main metabolites with the same retention time, and their structure was elucidated as 15β-hydroxy-RSS (Fig. S3g, h). In the case of CYP106A1, additional minor products appeared downstream the main product, increasing over time, together with the decrease of the main metabolite (Fig. S3g, h). From these, G1, with identical retention time to H2 produced by CYP106A2, was obtained in sufficient purity and quantity to be elucidated and turned out to be the 7β,15β-dihydroxy-RSS (Fig. S3g, h).

CYP106A1 reached 38 % in vivo cortisol conversion within 4 h. After 24 h, the substrate was entirely converted, but the product distribution seen in the in vitro study was completely altered. The products had the same retention times, but the in vivo observed ratios (I5 4 % and I6 20 %) were lower (Fig. 1i) compared with the in vitro results (I5 22 % and I6 28 %) (Fig. 1i). The main product (I6) of this newly identified CYP106A1 substrate was characterized as 11-dehydrocortisol (cortisone). CYP106A2 showed lower activity toward cortisol

with only 16 % conversion within 4 h and no complete substrate consumption even after 24 h. Unlike the product distribution in vitro (Fig. 1j), here, J1 was present as main product (Fig. S3j). However, CYP106A2 also produced a minor metabolite (J4) with matching retention time to 11-dehydrocortisol (I6), which was suggested to be the 11-keto compound.

Regarding cortisone, CYP106A1 converted 80 % of the substrate, while CYP106A2 performed complete conversion within 8 h. Both enzymes produced the main metabolite as observed in vitro (K3 and L3), whose structure was elucidated as 15β-hydroxycortisone (Fig. S3k, l). In vivo, the highest 15β-hydroxy product formation was 14 % by CYP106A1 within 4 h, while in vitro, it reached 56 % (Fig. S3k). CYP106A2 produced 40 % of the 15β-hydroxy metabolite in 4 h, and two previously undetected minor metabolites were also observed, one showing the same retention time as K4, the other downstream L1 (Fig. S3l). A CYP106A1 product observed only in vivo, downstream K1 was also purified and characterized as the 6β-hydroxylated compound. Interestingly, the minor products from the previous cortisol conversion (I2, I5 for CYP106A1 and J1, J3 for CYP106A2, see Fig. S3k, l) showed the exact same retention times as the 6β-hydroxycortisone and 15β-hydroxycortisone. This suggests that their structures are identical and, consequently, that both enzymes convert cortisol to cortisone, but the resulting 11-*oxo*-steroid is further hydroxylated to its 6β-hydroxy and 15β-hydroxy derivatives.

Discussion

The present paper reveals that out of 23 steroids studied, 19 were successfully converted by the CYP106A subfamily members, with 13 novel substrates identified for CYP106A1, and 7 for CYP106A2. Thus, CYP106A1, similarly to CYP106A2, is a highly active steroid hydroxylase, with 19 identified steroid substrates. A focused steroid library was used to compare both the CYP106A subfamily members, including 14 steroids formerly tested with CYP106A2 and nine additional 3-*oxo*-steroids, derivatives of testosterone, corticosterone, and androstenedione with distinct functional groups at C11, C17, and C19 positions. Difference spectroscopy revealed similar binding behaviors for all steroids toward both, CYP106A1 and CYP106A2 (Table 1). Out of 23 steroids tested, only four, namely β-estradiol, estrone, pregnenolone and 17α-hydroxypregnenolone, do not shift the heme iron into the high-spin form. Interestingly, all four compounds are 3-hydroxy steroids, either having an aromatic A-ring or a double bond between C5 and C6 (Fig. 2). Why the other tested 3-hydroxy-Δ5 steroid, DHEA, was able to induce a type I shift with both enzymes, is subject of further investigations and cannot be explained at this point.

Although not inducing an alteration of the spin-state, pregnenolone and 17α-hydroxypregnenolone were converted with both enzymes, supporting previous observations that type I binding is not necessary for conversion (Ferrero et al. 2012; Girhard et al. 2010; Schmitz et al. 2014; Simgen et al. 2000). Interestingly, the similarly functionalized 3-*oxo*-steroids progesterone and 17α-hydroxyprogesterone, induced a type I shift and were also converted. It is possible that the lacking hydrogen bond acceptor in the pregnenolone structure leads to a much weaker binding to the heme iron, thus not being able to displace the water and shift the spectrum. In contrast, estrogens (β-estradiol, estrone) are most probably not bound by CYP106A1 and CYP106A2, because no type I shift and no conversion have been observed for either substance. A possible explanation can be the lower flexibility of the aromatic A-ring, interfering with the binding of the substrate (Fig. 2) (Schmitz et al. 2014).

Although 3-*oxo*-Δ4-steroids are described as suitable substrates of CYP106A2, no conversion was observed for either 19-hydroxyandrostenedione or adrenosterone. These steroids have nearly identical structure to androstenedione (which is converted by both CYP106A enzymes) beside the hydroxyl group at C19 position and the keto-function at C11 position, respectively (Fig. 3). This suggests that these additional functional groups (perhaps in combination with other structural properties present on the steroid molecule) are responsible for disabling the conversion.

Interestingly, the substrate spectrum was the same for both enzymes, although the activities and product patterns were not alike in several cases. Focusing on the identification of differences between the CYP106A enzymes, the 19 substrates were narrowed down to those 6, whose conversion resulted in different product patterns or changed activities (Table 4). As a first step, the dissociation constants of these six substrates (androstenedione, corticosterone, DOC, RSS, cortisol, and cortisone) were determined. Steroid binding turned out to be similar with both CYP106A subfamily members, reflected by similar dissociations constants (Table 3). Strongest binding with both enzymes is observed for androstenedione (77 ± 2 μM with

Fig. 2 Investigated 3-hydroxy steroids, not inducing any spectral shift with either of the CYP106A subfamily members, except for dehydroepiandrosterone, showing a type I shift and conversion with both enzymes
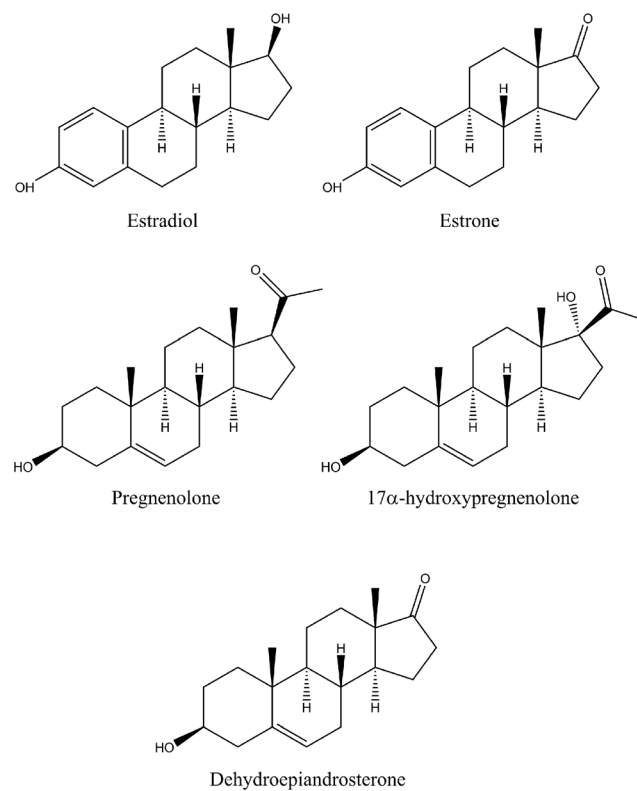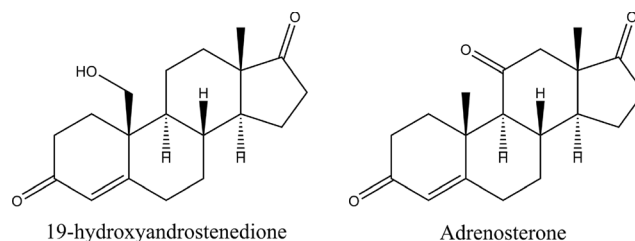

Estradiol

Estrone

Pregnenolone

17α-hydroxypregnenolone

Dehydroepiandrosterone

Fig. 3 Derivatives of the CYP106A-substrate androstenedione, which induce a type I shift, but show no conversion

19-hydroxyandrostenedione

Adrenosterone

CYP106A1 and 81±10 μM with CYP106A2) and DOC (68±2 and 50±1 μM, respectively), while the other chosen substrates with a functional group either at C11 or C17 show a rather weak interaction. Corticosterone and cortisone bind stronger to CYP106A2, whereas cortisol binds stronger to CYP106A1. However, the differences are within one order of magnitude and, therefore, relatively small. Unfortunately, the role of the CYP106A enzymes in *B. megaterium*—whose knockout is not lethal, but leads to significantly reduced growth rates—is a question that remains to be solved. Most likely CYP106A enzymes play a role in the growth of *B. megaterium* strains on alternative carbon and energy sources such as steroids and terpenoids. This assumption is supported by the fact that endogenous CYP106A2 is expressed only in the stationary phase of growth, when carbon and energy sources are depleted in the medium (Berg and Rafter 1981).

To obtain the hydroxylation products in sufficient amounts for NMR studies, whole-cell biotransformations were performed and the product structures elucidated (Table 4). Both enzymes favored the 15β-position when using C21-steroids such as DOC, RSS, and cortisone. However, differences were observed with corticosterone and androstenedione. In the case of corticosterone, the main product was 11-dehydrocorticosterone using CYP106A1, while for CYP106A2 the main product was identified as 15β-hydroxycorticosterone. Androstenedione was hydroxylated at position 15β by CYP106A2 and both at positions 6β and 7β with CYP106A1.

In order to get insight into the differences in steroid conversion between the CYP106A enzymes, an alignment was performed, where all conserved features of P450s were recognized in both enzymes (Table 4). Focusing on the substrate recognition sites (SRS), previously identified by Gotoh (1992), the SRS1 and SRS4-6 regions of CYP106A1 showed considerable differences in the amino acid pattern from the ones present in CYP106A2 (Fig. 4). The different residues in the SRS1 region, being responsible for the final stabilization of the substrate in the active site and in the SRS4-6 regions, involved in the initial substrate recognition and binding, could provide an explanation for the different regioselectivity and stereoselectivity of the isoenzymes. We also examined the hΦ-Pro motif in SRS1, where a hydrophobic residue precedes the amino acid proline before the B'helix, which is usually associated with high substrate selectivity or regiospecificity and stereospecificity (Pochapsky et al. 2010). In CYP106A2, the hydrophobic residue is valine at position 82, followed by the proline, while in CYP106A1, position 82 is occupied by a threonine, followed by a serine. This difference might contribute to the lower selectivity of CYP106A1. In case of androstenedione, for instance, CYP106A2 hydroxylates the C-ring at position 15β preferentially, whereas CYP106A1 attacks at the B-ring with less selectivity resulting in 6β-hydroxysteroids and 7β-hydroxysteroids as main products.

Fig. 4 Alignment of the amino acid sequences of CYP106A1 and CYP106A2, showing the SRS regions identified by Gotoh (1992). The identical residues in the SRS region are shown in *light blue*, the different ones shown in *red*, and the residues identified as lining the CYP106A2 active site by Janocha (2013) are marked with *dark blue*. The hΦ-Pro motif is shown with a *blue frame*

Both enzymes hydroxylated the steroids mainly at the C-rings and B-rings. However, in the case of steroids with a hydroxyl group at C11, a completely different reaction was observed. The CYP106A1 enzyme enabled the dehydrogenation of cortisol and corticosterone, whereas CYP106A2 performed the same reaction only with corticosterone, converting these 11β-hydroxysteroids into their 11-keto forms (Scheme 1). This reaction was not yet described for the CYP106A subfamily and was only suggested to occur in one other case of P450s (Suhara et al. 1986). The mechanism is still unidentified and a highly interesting topic for further research. Yet, a very similar oxidation mechanism was studied by Bellucci et al., where the model reaction was the oxidation of an allylic alcohol, and by Matsunaga et al., where the oxidation mechanism of hydroxy-Δ^8-tetrahydrocannabinols was investigated. Both studies concluded that the so-called *gem*-diol pathway could be an explanation of the mechanism, while as an alternative, they proposed a combination of the *gem*-diol and the double hydrogen abstraction pathway (Bellucci et al. 1996; Matsunaga et al. 2001).

Besides the reaction mechanism, the transformation of cortisol to cortisone is also notable, since both steroid hormones have important roles as pharmaceutical agents (Carballeira et al. 2009). Although, the 11-oxidase reaction catalyzed by CYP106A1 has shown only 19 % selectivity toward cortisone formation, we are confident that following the optimization of the *B. megaterium* whole-cell system, in combination with enzyme engineering tools, the selectivity of the enzyme could be increased toward an alternative route for this reaction.

In summary, in this work, we extended the substrate range of the CYP106A subfamily, identifying 13 new steroidal substrates for CYP106A1 and 7 for CYP106A2. The enzymes produced hydroxylated metabolites at positions 6β, 7β, 9α, and 15β and showed furthermore an unprecedented 11-oxidase activity. The hydroxyl groups introduced selectively in the steroid backbone make these derivatives valuable for the pharmaceutical industry. Either used as standards for human drug metabolites or as drug precursors for further functionalization, the production of these compounds with the help of the CYP106A subfamily has undoubtable advantage over chemical approaches. Our results strongly support the importance of the CYP106A1 and CYP106A2 enzymes for the pharmaceutical industry, especially for the production of human drug metabolites and drug precursors.

References

Agematu H, Matsumoto N, Fujii Y, Kabumoto H, Doi S, Machida K, Ishikawa J, Arisawa A (2006) Hydroxylation of testosterone by bacterial cytochromes P450 using the *Escherichia coli* expression system. Biosci Biotechnol Biochem 70(1):307–311

Barg H, Malten M, Jahn M, Jahn D (2005) Protein and vitamin production in *Bacilllus megaterium* Microbial processes and products, vol 18, 1st edn. Humana, Totowa, pp 205–223

Bellucci G, Chiappe C, Pucci L, Gervasi PG (1996) The mechanism of oxidation of allylic alcohols to α, β-unsaturated ketones by cytochrome P450†. Chem Res Toxicol 9(5):871–874

Berg A, Rafter JJ (1981) Studies on the substrate specificity and inducibility of cytochrome P-450meg. Biochem J 196(3):781–786

Berg A, Gustafsson J, Ingelman-Sundberg M (1976) Characterization of a cytochrome P-450-dependent steroid hydroxylase system present in *Bacillus megaterium*. J Biol Chem 251:2831–2838

Berg A, Ingelman-Sundberg M, Gustafsson J (1979) Isolation and characterization of cytochrome P-450meg. Acta Biol Med Ger 38:333–344

Bernhardt R (2006) Cytochromes P450 as versatile biocatalysts. J Biotechnol 124(1):128–145

Bernhardt R, Urlacher V (2014) Cytochromes P450 as promising catalysts for biotechnological application: chances and limitations. Appl Microbiol Biotechnol 98(14):6185–6203

Bleif S, Hannemann F, Lisurek M, Kries J, Zapp J, Dietzen M, Antes I, Bernhardt R (2011) Identification of CYP106A2 as a regioselective allylic bacterial diterpene hydroxylase. Chem Biol Chem 12:576–582

Bleif S, Hannemann F, Zapp J, Hartmann D, Jauch J, Bernhardt R (2012) A new *Bacillus megaterium* whole-cell catalyst for the hydroxylation of the pentacyclic triterpene 11-keto-beta-boswellic acid (KBA) based on a recombinant cytochrome P450 system. Appl Microbiol Biotechnol 93:1135–1146

Bracco P, Janssen D, Schallmey A (2013) Selective steroid oxyfunctionalisation by CYP154C5, a bacterial cytochrome P450. Microb Cell Fact 12(1):95

Brill E (2013) Identifizierung und Charakterisierung neuer Cytochrom P450 Systeme aus *Bacillus megaterium* DSM319 Universität des Saarlandes

Brill E, Hannemann F, Zapp J, Bruning G, Jauch J, Bernhardt R (2014) A new cytochrome P450 system from *Bacillus megaterium* DSM319 for the hydroxylation of 11-keto-beta-boswellic acid (KBA). Appl Microbiol Biotechnol 98:1701–1717

Carballeira JD, Quezada MA, Hoyos P, Simeó Y, Hernaiz MJ, Alcantara AR, Sinisterra JV (2009) Microbial cells as catalysts for stereoselective red–ox reactions. Biotechnol Adv 27(6):686–714

Chefson A, Auclair K (2006) Progress towards the easier use of P450 enzymes. Mol Biosyst 2(10):462–469

Choudhary MI, Sultan S, Khan MTH, Rahman A-u (2005) Microbial transformation of 17α-ethynyl- and 17α-ethylsteroids, and tyrosinase inhibitory activity of transformed products. Steroids 70(12): 798–802

Choudhary MI, Erum S, Atif M, Malik R, Khan NT, Attaur R (2011) Biotransformation of (20S)-20-hydroxymethylpregna-1,4-dien-3-one by four filamentous fungi. Steroids 76(12):1288–1296

Donova M, Egorova O (2012) Microbial steroid transformations: current state and prospects. Appl Microbiol Biotechnol 94:1423–1447

Ewen K, Ringle M, Bernhardt R (2012) Adrenodoxin—a versatile ferredoxin. IUBMB Life 64:506–512

Faramarzi MA, Tabatabaei Yazdi M, Amini M, Zarrini G, Shafiee A (2003) Microbial hydroxylation of progesterone with *Acremonium strictum*. FEMS Microbiol Lett 222(2):183–186

Ferrero VEV, Di Nardo G, Catucci G, Sadeghi SJ, Gilardi G (2012) Fluorescence detection of ligand binding to labeled cytochrome P450 BM3. Dalton Trans 41(7):2018–2025

Girhard M, Klaus T, Khatri Y, Bernhardt R, Urlacher V (2010) Characterization of the versatile monooxygenase CYP109B1 from *Bacillus subtilis*. Appl Microbiol Biotechnol 87(2):595–607

Gotoh O (1992) Substrate recognition sites in cytochrome P450 family 2 (CYP2) proteins inferred from comparative analyses of amino acid and coding nucleotide sequences. J Biol Chem 267(1):83–90

Hannemann F, Virus C, Bernhardt R (2006) Design of an *Escherichia coli* system for whole cell mediated steroid synthesis and molecular evolution of steroid hydroxylases. J Biotechnol 124(1):172–181

Hannemann F, Bichet A, Ewen KM, Bernhardt R (2007) Cytochrome P450 systems—biological variations of electron transport chains. Biochim Biophys Acta 1770(3):330–344

He J, Ruettinger R, Liu H, Fulco A (1989) Molecular cloning, coding nucleotides and the deduced amino acid sequence of P-450BM-1 from *Bacillus megaterium*. Biochim Biophys Acta 1009(3):301–303

He J, Liang Q, Fulco A (1995) The molecular cloning and characterization of BM1P1 and BM1P2 proteins, putative positive transcription factors involved in barbiturate-mediated induction of the genes encoding cytochrome P450BM-1 of *Bacillus megaterium*. J Biol Chem 270:18615–18625

Hollmann F, Hofstetter K, Schmid A (2006) Non-enzymatic regeneration of nicotinamide and flavin cofactors for monooxygenase catalysis. Trends Biotechnol 24(4):163–171

Janeczko T, Dmochowska-Gładysz J, Kostrzewa-Susłow E, Białońska A, Ciunik Z (2009) Biotransformations of steroid compounds by *Chaetomium* sp. KCH 6651. Steroids 74(8):657–661

Janocha S (2013) Umsatz von Harzsäuren durch die bakteriellen Cytochrome CYP105A1 und CYP106A2 – Strukturelle Grundlagen und potentielle Anwendungen. Saarländische Universitäts- und Landesbibliothek, Saarbrücken

Janocha S, Bernhardt R (2013) Design and characterization of an efficient CYP105A1-based whole-cell biocatalyst for the conversion of resin acid diterpenoids in permeabilized *Escherichia coli*. Appl Microbiol Biotechnol 97:7639–7649

Khatri Y, Hannemann F, Girhard M, Kappl R, Même A, Ringle M, Janocha S, Leize-Wagner E, Urlacher V, Bernhardt R (2013) Novel family members of CYP109 from *Sorangium cellulosum* So ce56 exhibit characteristic biochemical and biophysical properties. Biotechnol Appl Biochem 60(1):18–29

Kirk DN, Toms HC, Douglas C, White KA, Smith KE, Latif S, Hubbard RWP (1990) A survey of the high-field ^{1}H NMR spectra of the steroid hormones, their hydroxylated derivatives, and related compounds. J Chem Soc Perkin Trans 2(9):1567–1594

Korneli C, David F, Biedendieck R, Jahn D, Wittmann C (2013) Getting the big beast to work—systems biotechnology of *Bacillus megaterium* for novel high-value proteins. J Biotechnol 163(2):87–96

Lee G-Y, Kim D-H, Kim D, Ahn T, Yun C-H (2014) Functional characterization of steroid hydroxylase CYP106A1 derived from *Bacillus megaterium*. Arch Pharm Res 1–10

Li Y, Drummond DA, Sawayama AM, Snow CD, Bloom JD, Arnold FH (2007) A diverse family of thermostable cytochrome P450s created by recombination of stabilizing fragments. Nat Biotechnol 25(9):1051–1056

Lisurek M, Kang M, Hartmann R, Bernhardt R (2004) Identification of monohydroxy progesterones produced by CYP106A2 using comparative HPLC and electrospray ionisation collision-induced dissociation mass spectrometry. Biochem Biophys Res Commun 319:677–682

Lisurek M, Simgen B, Antes I, Bernhardt R (2008) Theoretical and experimental evaluation of a CYP106A2 low homology model and production of mutants with changed activity and selectivity of hydroxylation. Chem Biol Chem 9:1439–1449

Makino T, Katsuyama Y, Otomatsu T, Misawa N, Ohnishi Y (2014) regio- and stereospecific hydroxylation of various steroids at the 16α position of the d ring by the *Streptomyces griseus* cytochrome P450 CYP154C3. Appl Environ Microbiol 80(4):1371–1379

Matsunaga T, Tanaka H, Higuchi S, Shibayama K, Kishi N, Watanabe K, Yamamoto I (2001) Oxidation mechanism of 7-hydroxy-δ8-tetrahydrocannabinol and 8-hydroxy-δ9-tetrahydrocannabinol to the corresponding ketones by CYP3A11. Drug Metab Dispos 29(11):1485–1491

Matsuzaki K, Arai T, Miyazaki T, Yasuda K (1995) Formation of 6β-OH-deoxycorticosterone from deoxycorticosterone by A6 cells. Steroids 60(7):457–462

Mineki S, Iida M, Kato K, Fukaya F, Kita K, Nakamura J, Yoshihama M (1995) Microbial production of hydroxy-C19-steroids as estrogen synthetase (P-450 aromatase) inhibitors. J Ferment Bioeng 80(3):223–228

Nguyen K, Virus C, Gunnewich N, Hannemann F, Bernhardt R (2012) Changing the regioselectivity of a P450 from C15 to C11 hydroxylation of progesterone. Chem Biol Chem 13:1161–1166

O'Reilly E, Kohler V, Flitsch SL, Turner NJ (2011) Cytochromes P450 as useful biocatalysts: addressing the limitations. Chem Commun 47(9):2490–2501

Omura T, Sato R (1964) The carbon monoxide-binding pigment of liver microsomes: I. Evidence for its hemoprotein nature. J Biol Chem 239:2370–2378

Pochapsky T, Kazanis S, Dang M (2010) Conformational plasticity and structure/function relationships in cytochromes P450. Antioxid Redox Signal 13(8):1273–1296

Sagara Y, Wada A, Takata Y, Waterman M, Sekimizu K, Horiuchi T (1993) Direct expression of adrenodoxin reductase in *Escherichia coli* and the functional characterization. Biol Pharm Bull 16:627–630

Schenkman J, Jansson I (1998) Spectral analyses of cytochromes P450. Methods Mol Biol (Clifton, NJ) 107:25

Schenkman J, Sligar S, Cinti D (1981) Substrate interaction with cytochrome P-450. Pharmacol Ther 12:43–71

Schmitz D, Zapp J, Bernhardt R (2012) Hydroxylation of the triterpenoid dipterocarpol with CYP106A2 from *Bacillus megaterium*. FEBS J 279:1663–1674

Schmitz D, Zapp J, Bernhardt R (2014) Steroid conversion with CYP106A2 — production of pharmaceutically interesting DHEA metabolites. Microb Cell Fact 13:81

Seng Wong T, Arnold FH, Schwaneberg U (2004) Laboratory evolution of cytochrome P450 BM-3 monooxygenase for organic cosolvents. Biotechnol Bioeng 85(3):351–358

Simgen B, Contzen J, Schwarzer R, Bernhardt R, Jung C (2000) Substrate binding to 15beta-hydroxylase (CYP106A2) probed by FT infrared spectroscopic studies of the iron ligand CO stretch vibration. Biochem Biophys Res Commun 269:737–742

Suhara K, Takeda K, Katagiri M (1986) P-45011β-dependent conversion of cortisol to cortisone, and 19-hydroxyandrostenedione to 19-*oxo*-androstenedione. Biochem Biophys Res Commun 136(1):369–375

Tong W, Dong X (2009) Microbial biotransformation: recent developments on steroid drugs. Recent Pat Biotechnol 3(2):141–153

Uhlmann H, Beckert V, Schwarz D, Bernhardt R (1992) Expression of bovine adrenodoxin in *E. coli* and site-directed mutagenesis of/2 Fe-2S/cluster ligands. Biochem Biophys Res Commun 188:1131–1138

Urlacher VB, Eiben S (2006) Cytochrome P450 monooxygenases: perspectives for synthetic application. Trends Biotechnol 24:324–330

Urlacher VB, Girhard M (2012) Cytochrome P450 monooxygenases: an update on perspectives for synthetic application. Trends Biotechnol 30:26–36

Urlacher VB, Lutz-Wahl S, Schmid RD (2004) Microbial P450 enzymes in biotechnology. Appl Microbiol Biotechnol 64:317–325

Vary P, Biedendieck R, Fuerch T, Meinhardt F, Rohde M, Deckwer W-D, Jahn D (2007) *Bacillus megaterium*—from simple soil bacterium to industrial protein production host. Appl Microbiol Biotechnol 76:957–967

Venkataraman H, te Poele E, Rosłoniec K, Vermeulen N, Commandeur JM, van der Geize R, Dijkhuizen L (2014) Biosynthesis of a steroid metabolite by an engineered *Rhodococcus erythropolis* strain expressing a mutant cytochrome P450 BM3 enzyme. Appl Microbiol Biotechnol 1–9

Virus C, Bernhardt R (2008) Molecular evolution of a steroid hydroxylating cytochrome P450 using a versatile steroid detection system for screening. Lipids 43:1133–1141

Virus C, Lisurek M, Simgen B, Hannemann F, Bernhardt R (2006) Function and engineering of the 15beta-hydroxylase CYP106A2. Biochem Soc Trans 34:1215–1218

Wittchen K, Meinhardt F (1995) Inactivation of the major extracellular protease from *Bacillus megaterium* DSM319 by gene replacement. Appl Microbiol Biotechnol 42:871–877

Zehentgruber D, Hannemann F, Bleif S, Bernhardt R, Lütz S (2010) Towards preparative scale steroid hydroxylation with cytochrome P450 monooxygenase CYP106A2. Chem Biol Chem 11:713–721